SMOKING, CHROMOSOME DAMAGE AND AN ABNORMAL DNA DAMAGE RESPONSE IN HEAD AND NECK SQUAMOUS CELL CARCINOMA (HNSCC)

by

Rafael Ernesto Flores Obando

Licenciatura, Clinical Bio Analysis, Universidad Nacional Autónoma de Nicaragua,

Nicaragua, 1996

Submitted to the Graduate Faculty of

the Graduate School of Public Health in partial fulfillment

Of the requirements for the degree of

Master of Science

University of Pittsburgh

2009

UNIVERSITY OF PITTSBURGH

GRADUATE SCHOOL OF PUBLIC HEALTH

This thesis was presented

by

Rafael Ernesto Flores Obando

It was defended on

May 29th, 2009

and approved by

Thesis Advisor:
Susanne M. Gollin, Ph.D.
Professor
Department of Human Genetics
Graduate School of Public Health
University of Pittsburgh

Committee Member:
Robert E. Ferrell, Ph.D.
Professor
Department of Human Genetics
Graduate School of Public Health
University of Pittsburgh

Committee Member:
William S. Saunders, Ph.D.
Associate Professor
Department of Biological Sciences
School of Arts and Sciences
University of Pittsburgh

Advisor: Susanne M. Gollin, Ph.D.

SMOKING, CHROMOSOME DAMAGE AND AN ABNORMAL DNA DAMAGE RESPONSE IN HEAD AND NECK SQUAMOUS CELL CARCINOMA (HNSCC)

Rafael Ernesto Flores Obando, M.S.

University of Pittsburgh, 2009

Smoking is one of the leading risk factors that contribute to the development of head and neck squamous cell carcinoma (HNSCC). Smoking induces chromosome breaks. One of the most frequent and earliest alterations in HNSCC is the segmental loss of the short arm of chromosome 3 (3p). Another frequent observation is the activation of one of the most common fragile sites in HNSCC, FRA3B, which spans the *FHIT* gene, considered to be a tumor suppressor. Distal to *FHIT* is *FANCD2*, which encodes a protein required for the proper function of the Fanconi anemia/BRCA pathway and eventual repair of DNA damage through homologous recombination repair. Recently, it has been observed that FANCD2 gene and protein expression is decreased in HNSCC cells. Therefore, we hypothesize that 3p loss, resulting from the activation of the fragile site FRA3B, leads to *FANCD2* gene copy loss and a defective DNA damage response. Western blots showed decreased expression of FHIT protein in HNSCC cell lines. Fluorescence *in situ* hybridization revealed partial loss of *FANCD2* in HNSCC cell lines studied. Western blotting and quantitative RT-PCR showed decreased FANCD2 protein and gene expression in HNSCC cell lines with *FANCD2* gene copy loss. HNSCC cell lines with decreased FHIT protein expression, *FANCD2* gene copy loss, and decreased *FANCD2* gene and protein expression exhibited decreased FANCD2 and RAD51 focus formation. Our results suggest that smoking could induce breakage of the fragile site, FRA3B, leading to *FANCD2* loss and resulting in defective DNA damage repair. The use of targeted therapy on cancer cells with

deficient DNA damage repair, like CHEK1 small molecule inhibitors, could improve the currently available cancer treatment schemes. The public health relevance of our studies involves the use of an abnormal FA/BRCA pathway as a marker for selective use of targeted cancer therapy for HNSCC.

TABLE OF CONTENTS

ACKNOWLEDGEMENTS XII

1.0 INTRODUCTION 1

1.1 SMOKING AND ALCOHOL IN HNSCC 1

1.2 FRAGILE SITES AND CHROMOSOMAL INSTABILITY IN HNSCC 2

1.3 FANCONI ANEMIA/BRCA PATHWAY 5

1.4 DNA DAMAGE RESPONSE AND FA/BRCA PATHWAY 9

1.5 CHEK1 INHIBITION AND RADIOSENSITIZATION 11

2.0 HYPOTHESIS AND AIMS 13

2.1 HYPOTHESIS 13

2.2 AIM 1 13

2.3 AIM 2 13

2.4 AIM 3 14

2.5 AIM 4 14

2.6 AIM 5 14

2.7 AIM 7 15

3.0 MATERIALS AND METHODS 16

3.1 CELL LINES AND CULTURE CONDITIONS 16

3.1.1 HNSCC cell lines 16

3.1.2 Controls 17
3.2 GENERATION OF DNA DAMAGE 17
3.3 FLUORESCENCE *IN SITU* HYBRIDIZATION 18
3.4 RNA EXTRACTION AND QUANTITATIVE REVERSE TRANSCRIPTASE PCR 19
3.5 IMMUNOBLOTTING 22
3.6 IMMUNOFLUORESCENCE MICROSCOPY 24
3.7 PREPARATION AND USE OF THE CHEK1 SMALL MOLECULE INHIBITOR (SMI) 25
3.8 CLONOGENIC SURVIVAL ASSAY 25
3.9 FLOW CYTOMETRY 27
4.0 RESULTS 28
4.1 CELL LINE DESCRIPTION 28
4.2 DECREASED FHIT PROTEIN EXPRESSION IN HNSCC CELL LINES 29
4.3 *FANCD2* GENE COPY NUMBER LOSS IN HNSCC CELL LINES 31
4.4 INDUCTION OF *FANCD2* GENE EXPRESSION IN RESPONSE TO MMC IS DECREASED IN HNSCC CELL LINES 33
4.5 FANCD2 PROTEIN EXPRESSION IS DECREASED IN HNSCC CELL LINES 35
4.6 DECREASED FANCD2 AND RAD51 FOCUS FORMATION IN HNSCC CELL LINES 39
4.7 HNSCC CELL LINES DO NOT SURVIVE 10 GY IR 44

4.8 DECREASED CELL SURVIVAL IN TP53 MUTANT HNSCC CELL LINES AFTER EXPOSURE TO THE CHEK1 SMI 48

4.9 THE CHEK1 SMI ABROGATES THE G2/M CHECKPOINT IN TP53-DEFICIENT HNSCC CELL LINES. 50

5.0 DISCUSSION 52

5.1 *FHIT* AND THE DEFECTIVE FA/BRCA PATHWAY IN HNSCC CELL LINES 52

5.2 CHEK1 INHIBITION AND A DEFECTIVE FA/BRCA PATHWAY IN HNSCC CELL LINES 59

6.0 PUBLIC HEALTH SIGNIFICANCE 63

BIBLIOGRAPHY 64

LIST OF TABLES

Table 1. Master Mix and Reverse Transcriptase reaction set-up. 20

Table 2. Master Mix for 2X TaqMan Buffer set-up. 21

Table 3. Master Mix for QPCR set-up. 21

Table 4. Characteristics of the patients and cell lines used in the study. 28

LIST OF FIGURES

Figure 1. The FHIT gene. 4

Figure 2. FA/BRCA pathway in response to DNA damage. 8

Figure 3. FHIT protein expression in HNSCC cell lines. 30

Figure 4. Loss of *FANCD2* gene copy number in fourteen HNSCC cell lines determined by FISH 32

Figure 5. FISH results for *FANCD2* compared to CEP3 33

Figure 6. FANCD2 baseline and induced expression in HNSCC cell lines with and without exposure to MMC. 35

Figure 7. Induced *FANCD2* gene expression in HNSCC cell lines upon exposure to 80 ng/ml MMC. 35

Figure 8. FANCD2 western blot of HNSCC cell lines. 37

Figure 9. Bar graph showing the percentage of HNSCC cells with FANCD2 foci. 40

Figure 10. Bar graph showing the percentage of HNSCC cells with RAD51 foci. 40

Figure 11. UPCI:SCC131 showing decreased FANCD2 and RAD51 focus formation. 41

Figure 12. UPCI:SCC142 showing decreased FANCD2 and RAD51 focus formation. 41

Figure 13. HNSCC derived from FA patient OHSU974 showing absence of FANCD2 and RAD51 focus formation. 42

Figure 14. FA/BRCA pathway proficient cell line HeLa exhibiting FANCD2 and RAD51 focus formation. 43

Figure 15. Graph showing the L/S ratio of FANCD2 monoubiquitination, quantitation of *FANCD2* gene expression, and cells percentage of FANCD2 focus formation. 44

Figure 16. Clonogenic survival assay on UPCI:SCC078 46

Figure 17. Clonogenic survival assay on UPCI:SCC099 after exposure to CHEK1 SMI and IR.47

Figure 18. Clonogenic survival assay on UPCI:SCC131 after exposure to CHEK1 SMI and IR.47

Figure 19. Clonogenic survival assay on UPCI:SCC136 after exposure to CHEK1 SMI and IR.48

Figure 20. Western blotting for (A) total TP53 and (B) phospho-TP53 (ser15) in UPCI:SCC078, 099, 116 and 131 untreated and treated with 80 ng/ml MMC. 49

Figure 21. Cell cycle analysis of (A) UPCI:SCC078 (TP53 wild-type) and (B) 099 (TP53-mutant) treated and untreated with 5 Gy and 180 nM of CHEK1 SMI. 51

Figure 22. RAD9 protein expression in HNSCC cell lines and the HEK293 cell line. 59

ACKNOWLEDGEMENTS

First, I would like to thank God for leading every step of my life, for allowing me to understand and experience what cancer is all about, and for giving me the strength and the courage to pursue every one of my dreams.

I would like to thank my academic advisor, Dr. Susanne M. Gollin, who gave me the opportunity of working in her laboratory, for allowing me to work in Head and Neck cancer and for providing me her support when I needed it the most. To my committee members, Dr. Robert E. Ferrell and Dr. William Saunders, for allotting some time out of their busy schedules to provide guidance and ideas to my research work. To the current and former Gollin Lab family members: Mr. Dale Lewis, Dr. Brian Henson, Dr. Xin Huang, Steve Seasholtz, Madhav Sankunny, and Jianhua Zhou for their invaluable discussions and support in the lab.

I would like to thank Fulbright/IIE for awarding me the scholarship that made it possible for me to come to the University of Pittsburgh to conduct my graduate studies.

I would like to thank my parents and my brothers for their unconditional support.

Finally, I would like to thank my family, wife Karla, my daughter Dana, and my son Jonas, for being patient with me and for being by my side during this amazing educational adventure. They are my source of inspiration and dedication.

1.0 INTRODUCTION

Head and neck squamous cell carcinoma (HNSCC) represents a disease with a high public health impact considering that at least 80% of the oral cancers are attributed to cigarette smoke and alcohol consumption (Haddad and Shin 2008; Negri, et al. 1993). This is quite disturbing for a disease that is the eight most common cancer worldwide, with approximately 650,000 new cases every year (Jemal, et al. 2008) - around 46,000 new cases reported in the United States during 2007 only (Parkin, et al. 2005) - and 5-year survival rates decreasing from 49.2% to 43.8% during the last 20 years (Carvalho, et al. 2005). These figures demand a continuous investigative effort to unravel the intricate nature of this type of cancer in order to come up not only with alternative treatments but also with novel preventive measures to decrease its appearance in the most susceptible groups of the population.

1.1 SMOKING AND ALCOHOL IN HNSCC

Cigarette smoke and alcohol are the top risk factors in the development of HNSCC. Even though cigarette smoke or alcohol consumption represent a risk factor alone (Talamini, et al. 1990; Talamini, et al. 1998), the risk is greater (around 13-fold) in those individuals exposed to both cigarette smoke (more than 20 cigarettes per day) and alcohol (more than 5 drinks per day) at the same time (Castellsague, et al. 2004). The increased risk that comes about to those individuals

exposed to smoking and drinking and those who, on the other hand, get exposed to second hand smoke may be related to genetic polymorphisms in enzymes, like cytochrome p450 (e.g. CYP1A1, CYP2E1), glutathione S-transferase, UDP-glucuronosyltransferase and alcohol dehydrogenase (ADH) that detoxify tobacco carcinogens and alcohol-related genotoxic metabolites, respectively (Varela-Lema, et al. 2008). The inability to eliminate tobacco carcinogens like polycyclic aromatic hydrocarbons and nitrosamines and alcohol genotoxic agents like acetaldehyde may lead to the formation of DNA adducts that interfere with DNA synthesis and repair (Olshan, et al. 2000; Poschl and Seitz 2004). This brings the gene-environmental interaction component to play in the genesis of HNSCC.

1.2 FRAGILE SITES AND CHROMOSOMAL INSTABILITY IN HNSCC

HNSCC is often characterized by chromosome instability which has been correlated with exposure to cigarette smoke and alcohol consumption (Reshmi and Gollin 2005; Wang, et al. 2008), resulting in the activation of fragile sites, deletion of tumor suppressor genes like *TP53,* and amplification of oncogenes like *CCND1* (Wang, et al. 2008). Cigarette smoke can activate one of the most commons fragile sites, FRA3B (Stein, et al. 2002). Fragile sites are specific loci that exhibit chromosome instability, visible as gaps and breaks on metaphase chromosomes following partial inhibition of DNA synthesis. Fragile sites can be divided into two groups: the rare fragile sites, also known as the folate-sensitive group, because they can be induced by folate deprivation from the cells in culture and are frequently associated with CGC repeat expansions. FRAXE and FRAXA belong to this group. The other group is known as common fragile sites, which can be induced by aphidicolin. The common fragile sites differ from the rare fragile sites

in that they are part of the normal chromosomal structure and are not formed by nucleotide expansion repeats. One of the best studied common fragile sites most studies is FRA3B (Durkin and Glover 2007). Located at 3p14.2, FRA3B breakage may result in a segmental aberration involving the short arm of chromosome 3 (3p), rather than whole arm loss (Tsui, et al. 2008). Deletion of 3p is frequently observed in human cancers, including breast (60%) (Matsumoto, et al. 1997), lung (96%) (Wistuba, et al. 2000), cervical (40-70%) (Holschneider, et al. 2005), and HNSCC (45-55%) (Virgilio, et al. 1996). Initially identified by positional cloning and FISH, FRA3B, is a large genomic region characterized by genomic breakage and instability. FRA3B size ranges from the t(3;8) breakpoint to a region at least 500 Kb telomeric (Le Beau, et al. 1998). FRA3B activation is accompanied by the deletion of part of the fragile histidine triad gene (*FHIT*). *FHIT* is considered to be a tumor suppressor gene because it has been found in a genomic region that was homozygously deleted. *FHIT* deletion has included exons (between exon 5 and 9), which leads to aberrant transcripts frequently identified in human tumors (Le Beau, et al. 1998). Despite these observations, the role of *FHIT* as a classical tumor suppressor gene remains to be proven. It is because of the observation that cancer cells with aberrant *FHIT* transcripts are able to translate a functional form of the FHIT protein (Le Beau, et al. 1998). Decreased FHIT protein expression is common in human cancers (Huebner and Croce 2003), including breast (Yang, et al. 2001), lung (Sasaki, et al. 2006), cervix (Holschneider, et al. 2005), and HNSCC (Guerin, et al. 2006; Lee, et al. 2001; Virgilio, et al. 1996). The 1.7 MB *FHIT* gene, distributed over ~ 500 Kb, encodes a 1.2 kb mRNA and a 16.8 kDa protein. The *FHIT* gene is comprised of 10 exons. Exons 3, 4 (the first to be encoded) and 5 are proximal to translocation sites, like the t(3,8) and fragile sites, like the HPV integration site and the plasmid pVS2 (Figure 1). Maestro showed that there are three commonly deleted regions at 3p (3p24-pter, 3p21.3, and

3p14-cen), which were suggested to be involved in the genesis and/or progression of HNSCC (Maestro, et al. 1993). Sequence analysis of the aberrant RT-PCR products showed that absence of exon 4 or 5 through exon 8 was the most common abnormality. Absence of exon 8 is probably crucial, since it contains the highly conserved histidine triad motif and is essential for the function of the FHIT protein. Absence of exon 4, leaving the starting ATG in exon 5 untouched, resulted in transcripts with the potential to produce intact FHIT proteins (Druck, et al. 1997).

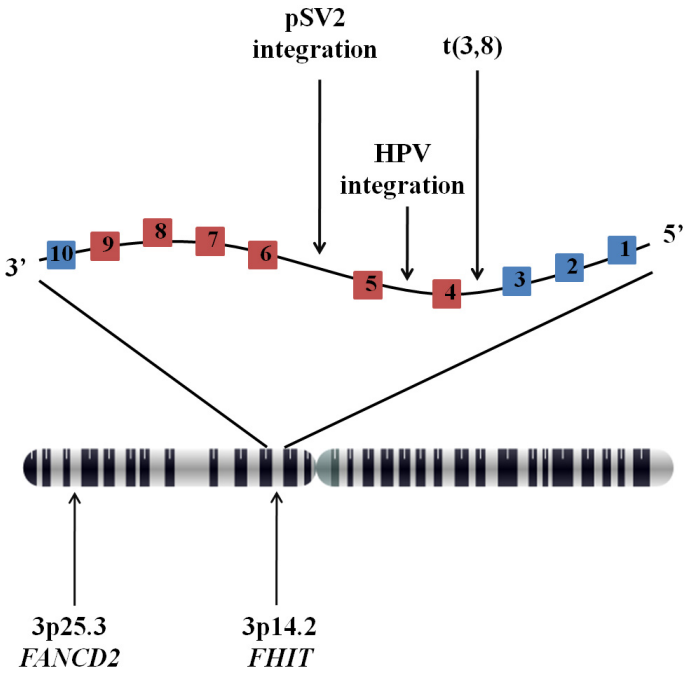

Figure 1. The FHIT gene.

The FHIT locus at 3p14.2 showing untranslated exons exons in blue. The FHIT protein coding exons are labeled in red. The image was modified from Huebner (Huebner, et al. 1997).

FANCD2, an important gene in the Fanconi anemia/BRCA (FA/BRCA) pathway is located at 3p25.3 (Hejna, et al. 2000), distal to FRA3B. Decreased FANCD2 gene and protein expression have been reported in head and neck cancer (Sparano, et al. 2006; Van Der Heijden,

et al. 2004; Wreesmann, et al. 2007). Furthermore, it has been shown that cigarette smoke condensate (CSC) equivalent to 20 cigarettes inhibits FANCD2 protein translation and monoubiquitination in bronchogenic carcinoma cells (Hays, et al. 2008). As a consequence, a defective FA/BRCA pathway leads to increased chromosomal instability (Hays, et al. 2008). This raises the question whether there is a possible interrelationship between cigarette smoking, fragile site breakage and DNA damage repair, particularly involving the Fanconi anemia/BRCA pathway.

1.3 FANCONI ANEMIA/BRCA PATHWAY

Fanconi anemia (FA) is a heterogeneous disease at both the phenotypic and genetic levels. Patients with FA present bone marrow failure, acute myelogenous leukemia (AML), skeletal abnormalities, defective DNA damage response, and high susceptibility to DNA cross-linking agents like mitomycin C (MMC). This leads to an increased predisposition to hematological and solid cancers, like acute myeloid leukemia and head and neck cancer, respectively. According to Rosenberg et al., FA patients have around a 50-fold increased risk for developing cancer in general and a 700-fold increased risk for developing head and neck cancer in comparison to the general population (Rosenberg, et al. 2008; Rosenberg, et al. 2003).

To date, 13 FA genes have been identified and the pathway can be divided into three major components: the core complex (FANCA, B, C, E, F, G, L, M), the ID complex (FANCD2 and FANCI) and the repair complex (FANCD1, FANCJ and FANCN) (Figure 2). Exposure to DNA inter-strand crosslinking agents like MMC leads to stalled replication forks allowing time for DNA damage repair. This alteration is recognized by the recombination protein A (RPA)

which coats the stalled replication sites or DNA damage site, activating ATR. This leads to the subsequent CHEK1 activation by phosphorylation. This is required to phosphorylate downstream targets in the FA core complex like FANCM, FANCE and FAAP-24. Alteration of any of the components of the FA core complex can halt the function of the whole pathway by preventing the monoubiquitination of FANCD2 and FANCI and the further assembly of the repair complex at the site of damage. The sensing of the DNA damage and further accumulation of core complex proteins at the DNA damage site depends on the phosphorylation of core complex members like FANCM, FAAP-24 and FANCE. FANCM has been suggested to have translocase activity that allows it to serve as a platform while recruiting and translocating the core complex to the site of DNA damage. The Fanconi associated protein 24 (FAAP24) is another component of the core complex. Interaction of FAAP24 with FANCM is required for the proper assembly of the core complex. This follows from the observation that in FAAP24-deficient cells, the core complex fails to assemble and load onto the DNA damage site. At some point, FANCE is also phosphorylated by CHEK1, who was previously phosphorylated by ATR, mediating the interaction between the core complex and the ID complex, specifically FANCD2. As a consequence, FANCD2 and FANCDI are translocated to the DNA damage site and get ubiquitinated by FANCL, which provides the ubiquitin E3 ligase activity. This step is also fueled by the phosphorylation of FANCD2 and FANCI by ATR or ATM. The activation of FANCD2 by ATR occurs in response to the stalled replication fork or DNA interstrand crosslinks. ATM also activates FANCD2 in response to IR.

The BRAFT complex, constituted by proteins like BLM helicase, topoisomerase III alpha, and replication protein A (RPA) also interact with the FA/BRCA. This is because the BLM helicase shows in vitro activity of branched DNA structures, which can occur during repair

of stalled replication fork by homologous recombination. The relocation of FANCD2 to the damage site depends on its interaction with BRCA1, an integral core complex and γ-H2AX, the phosphorylated version of H2AX. Ultimately, FANCD2 relocation to the site of DNA damage brings along homologous repair-associated proteins like BRCA1, BRCA2 (FANCD1), and RAD51 as well as protein members of the non-homologous end joining pathway like NBS1, the BLM helicase and partially other FA proteins like FANCE, FANCC and FANCJ enabling subsequent DNA damage repair. The observation that DNA repair factors like BRCA2 and PALB2 and mutated in FANCD1 and FANCN complementation groups, plus increased observe sensitivity of these complementation groups to DNA interstrand crosslinks, has created the notion that FA/BRCA pathway plays a critical role in repairing lesions that affect DNA replication through homologous recombination (Green and Kupfer 2009).

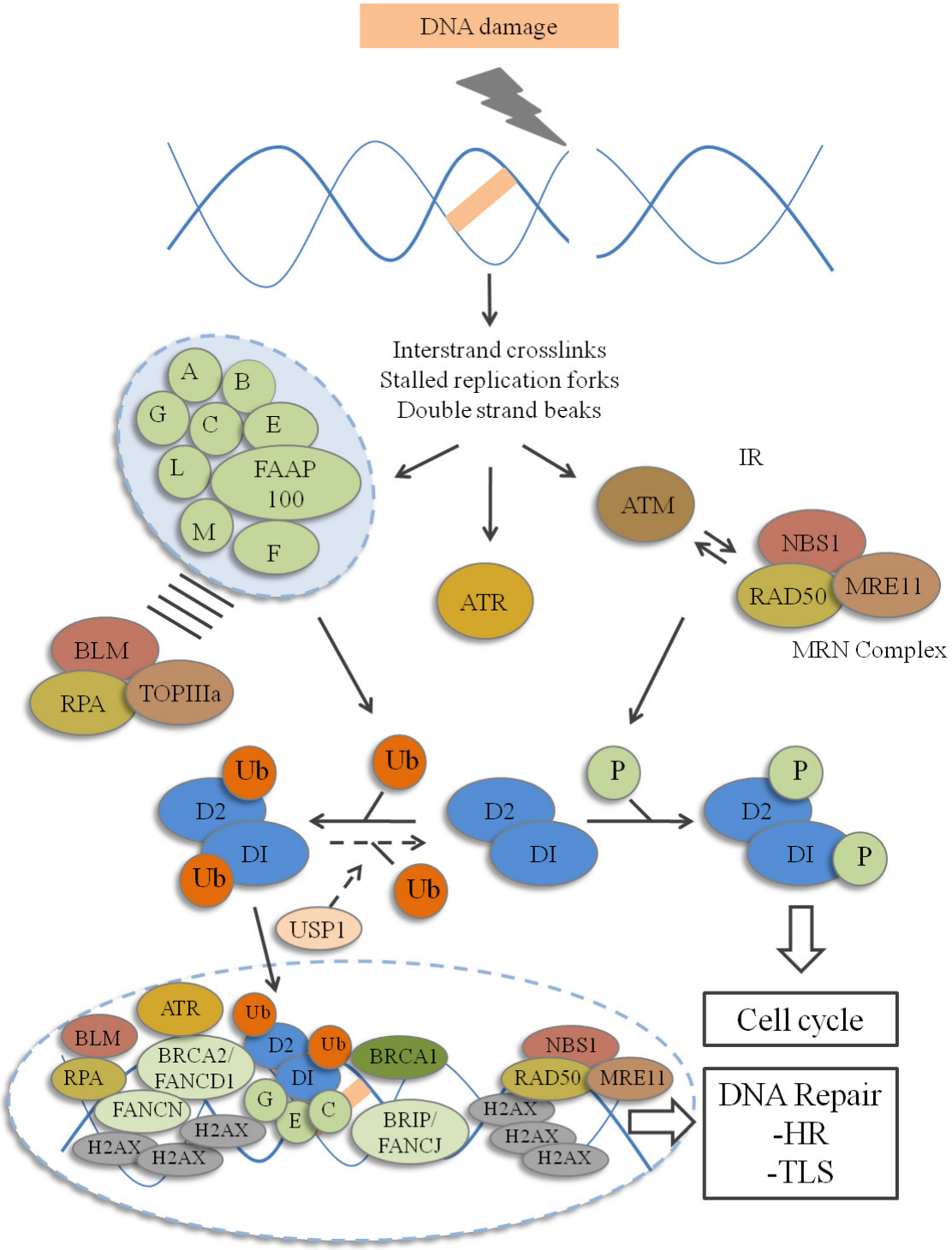

Figure 2. FA/BRCA pathway in response to DNA damage.

For explanations see the text, Fanconi anemia/BRCA pathway. The image was modified from Kalb (Kalb R 2007).

1.4 DNA DAMAGE RESPONSE AND FA/BRCA PATHWAY

The cells can be exposed to exogenous DNA damage agents (like IR and DNA inter-strand crosslinking agents) and endogenous agents (like species oxygen reactive products, meiotic recombination and stalled replication forks). The mechanism by which the DNA damage is sensed relies in a cooperative interaction between ATR and ATM through one of two ways: (1) a rapid cyclin dependent kinase (CDK)-independent or (2) a slow cyclin dependent kinase (CDK)-dependent pathway. The rapid, CDK-independent sensing is conducted by the MRN (MRE11 – RAD50 – NBS1) complex which primarily recognizes double strand breaks (DSB). Later, the MRN complex interacts with ATM through protein-protein interaction of the C-terminal motif of NBS1 and the HEAT repeats of ATM, leading to ATM autophosphorylation on serine residues S1981, S367 and S1893. Following the incorporation of the MRN-ATM complex to the DSB, ATM phosphorylates the C-terminus of histone H2AX, yielding γ-H2AX, which is used as platform for MDC1 (mediator of DNA damage checkpoint 1). The latter, which has a dual interaction with γ-H2AX and NBS1, leads to the spreading of the H2AX phosphorylation around the DSB site to further incorporate other DNA damage components like 53BP1 (TP53 binding protein 1, an important mediator of DNA damage signaling), BRCA1 (breast cancer 1 gene, necessary for the activation of CHEK1 during DNA damage-induced intra-S or G2 arrest), and the MRN complex itself. Finally, ATM phosphorylation further activates downstream targets like CHEK2, which helps in spreading the DNA damage signal throughout the nucleus, leading to cell cycle arrest (Bartek and Lukas 2007).

The MRN complex and ATM are also required to activate the slow, CDK-dependent kinase sensing of DNA damage. MRN and ATM initiate DSB resection and formation of ssDNA (single-strand DNA), a required structural intermediate for ATR-dependent signaling, which is

restricted to the S and G2 phases only. ssDNA is then coated by RPA which also binds ATRIP (ATR-interacting protein), facilitating the recognition of downstream phosphorylation targets like RAD9 and RAD17, required for further checkpoint signaling. The fully active ATR requires the DNA topoisomerase II-beta binding protein 1(TOPBP1), which is recruited to the ssDNA, for the phosphorylation of downstream targets, particularly CHEK1. CHEK1 phosphorylation and activation requires Claspin, a phosphorylation mediator protein, which is also requires for the ATR-dependent phosphorylation of RAD17 (Bartek and Lukas 2007).

The three major checkpoints of the cell cycle are: G_1/S, intra-S and G_2/M. The G_1/S checkpoint is characterized by activation of TP53, a key player in this checkpoint, which induces the expression of p21 and the consequent inhibition of the cyclin E-CDK2 complex. This event disrupts the interaction between TP53 and its negative regulator MDM2. MDM2 has ubiquitin ligase activity that allows the ubiquitination of TP53 and MDM2 itself, leading to their degradation by the proteasome pathway. Upon exposure to DNA damage, ATM phosphorylates TP53 at serine 15 (Ser-15) disrupting its interaction with MDM2, and allowing TP53 accumulation. Later, ATM also phosphorylates CHK2 on threonine 68 (Thr-68) allowing its interaction with TP53, essential for G_1 arrest. The intra-S checkpoint can be activated by either of two ways: first, once activated by ATM, CHEK2 phosphorylates CDC25A on serine 123 (Ser-123). CDC25C is a phosphatase required for DNA synthesis and activation of CDK2 by dephosphorylation of threonines 14 and 15 (Thr-14 and 15), leading to its degradation by the proteasome pathway and a stoppage of the S-phase. Alternatively, CHEK1 can be also involved in S-phase arrest through its ability to phosphorylate CDC25A. Second, the MRN complex can participate in S-phase arrest through the phosphorylation of NBS1 on serine 343 (Ser-343) by ATM. This event is required for the phosphorylation of SMC, part of the cohesion complex, on

serine 957 and 966 (Ser-957 and 966) contributing to the cohesion of sister chromatids, required for intra-S checkpoint activation. The activation of the G_2 checkpoint is accomplished by phosphorylation of CHEK1 on serines 317 and 345 (Ser-317 and 345) by either ATM or ATR. Later, CHEK1 phosphorylates CDC25C (a mitosis-promoting phosphatase) on serine 217 (Ser-217), resulting in binding with the 14-3-3 protein complex which prevents CDC25C dephosphorylation and further activation of the mitotic kinase cyclin B-CDK2. This blocks the cells with DNA damage from entering mitosis (Motoyama and Naka 2004).

The integrity of the FA/BRCA pathway is important for the activation of the DNA damage checkpoints to keep the cell from experiencing chromosomal instability. Depletion of CHEK1, which has FANCE as a phosphorylation target, induces chromosomal instability and breaks at common fragile sites in cancer cells (Durkin, et al. 2006). Furthermore, CHEK1-depleted cells exhibit decreased FANCD2 monoubiquitination upon exposure to DNA damage (Guervilly, et al. 2008). This supports the requirement of an intact CHEK1 to phosphorylate downstream targets like FANCE required for FANCD2 monoubiquitination and translocation to the damage site along with the DNA repair complex proteins. The application of CHK1 small molecule inhibitors (SMI) may affect the FA/BRCA pathway by inhibiting the phosphorylation of FA core complex targets, leading to defective DNA damage response.

1.5 CHEK1 INHIBITION AND RADIOSENSITIZATION

Based on our preliminary data, we have observed that OSCC cell lines with distal 11q loss have an increased resistance to ionizing radiation (Parikh, et al. 2007). The same observation was made on HNSCC cell lines with increased expression of *ATR* and *CHEK1* and loss of *TP53*

(Parikh, et al., unpublished data). Preliminary data suggest that inhibition of ATR or CHEK1 by siRNA resensitizes IR-resistant HNSCC cell lines to IR (Parikh, et al., unpublished data). A major effort is being made to develop SMI to facilitate the targeted inhibition of kinase activity for the treatment of cancer (Zhang, et al. 2009). Currently, there is a type-1 inhibitor, a CHEK1 SMI, that has ATP-competitive ability and recognizes the active conformation of the CHEK1 kinase in a TP53-dependent manner (Blasina, et al. 2008). Cancer cells lacking TP53, the major player in G1 checkpoint, retain intact S and G2/M checkpoints, which upon DNA damage, will allow them to arrest at such points giving them time for repair. Inhibiting CHEK1, critical for the function of the S and G_2/M checkpoints, is lethal for *TP53*-deficient cancer cells which have no time to repair DNA damage and are forced to enter mitosis with massive DNA damage. Therefore, CHEK1 SMI inhibits CHEK1 selectively in TP53-deficient cancer cells without disturbing the surrounding normal cells. In this way, CHEK1 SMI, currently in clinical trials to treat solid tumors in combination with chemotherapy, represents a promising compound for targeted therapy in cancer cells, like HNSCC, that overexpress CHEK1 with minimal side effects to the patient.

2.0 HYPOTHESIS AND AIMS

2.1 HYPOTHESIS

We hypothesize that HNSCC cell lines have altered *FANCD2* gene copy number, expression and/or monoubiquitination due to segmental loss of chromosomal arm 3p with a consequent decreased DNA damage response.

2.2 AIM 1

To determine the presence of FHIT protein expression in HNSCC cell lines.

Our hypothesis predicts that HNSCC cell lines will exhibit decreased FHIT expression compared to the positive control HEK293 cell line.

2.3 AIM 2

To determine *FANCD2* gene copy number in HNSCC cell lines.

Our hypothesis predicts that HNSCC cell lines with 3p loss will exhibit *FANCD2* copy number loss.

2.4 AIM 3

To assess *FANCD2* gene expression in HNSCC cell lines upon exposure to MMC.

Our hypothesis predicts that HNSCC cell lines with 3p loss will show decreased *FANCD2* gene expression compared to a FA/BRCA pathway proficient cell line upon exposure to MMC.

2.5 AIM 4

To determine whether FANCD2 is monoubiquitinated in HNSCC cell lines after exposure to MMC.

Our hypothesis predicts that HNSCC cell lines with 3p loss will show decreased FANCD2 monoubiquitination compared to a FA/BRCA pathway proficient cell line upon exposure to MMC.

2.6 AIM 5

To determine the ability of the HNSCC cell lines to induce FANCD2 focus formation after exposure to MMC.

Our hypothesis predicts that HNSCC cell lines will show decreased FANCD2 focus formation compared to a FA/BRCA pathway proficient cell line upon exposure to MMC.

2.7 AIM 7

To determine the effect of a CHEK1 small molecule inhibitor (SMI) in HNSCC cell lines after IR treatment.

In this aim, we used different doses of SMI to determine its effect in HNSCC cell lines after exposure to IR. The effect was measured by a clonogenic survival assay and cell cycle analysis.

3.0 MATERIALS AND METHODS

3.1 CELL LINES AND CULTURE CONDITIONS

We cultured 14 HNSCC cell lines established in the laboratory of Dr. Susanne M. Gollin, OHSU974 (HNSCC cell line derived from *FANCA* $^{-/-}$ patient established at the FA Cell Repository, at Oregon Health & Science University, Portland, OR), VU1365 (a HNSCC cell line derived from a *FANCA* $^{-/-}$ patient established at the Vrije University Medical Center, Amsterdam, The Netherlands), Human embryonic kidney 293 (HEK293) cells, and HeLa cells.

3.1.1 HNSCC cell lines

HNSCC cell lines were grown Minimal Essential Medium (Gibco Invitrogen), supplemented with 1% non-essential amino acids, 1% L-glutamine, 50 μg/ml gentamicin and 10% (v/v) FBS (FBS from Irvine Scientific Santa Ana, California, where all other supplements from Gibco Invitrogen, Carlsbad, CA). HNSCC cell lines were also grown in T25 flasks, incubated at 37°C in 5% CO_2 humidified incubator, and fed every 2 to 3 days. When 70 to 80% confluency was reached, the cells were subcultured (White, et al. 2007). The subculture of HNSCC cell lines was performed by rinsing HNSCC cell lines once in about 2 ml of 1X Hanks' Balanced Salt Solution

(HBSS; Irvine Scientific, Santa Ana, California). Then, 1.5 − 2 ml of 0.05% trypsin-0.02%EDTA (Gibco Invitrogen, Carlsbad, CA) was added to the flask to promote detachment of adherent cells. The flasks were incubated at 37°C in 5% CO_2 humidified incubator for no more than 5 min. During this time, the flasks were taken out of the incubator at least twice and were smacked to ease the detachment of the cells. Later, the trypsin was inactivated by the addition of M10 medium at a volume equal the initial amount of trypsin added to the flasks.

3.1.2 Controls

The OHS974 cell line (FA Cell Repository, Oregon Health & Science University, Portland, OR) was cultured under the same conditions as the HNSCC cell lines from Dr. Gollin's laboratory. The VU1365 cell line was cultured in Dulbecco's Modified Eagle Medium (DMEM) (Gibco Invitrogen, Carlsbad, CA), supplemented with 1% nonessential amino acids, 0.05 mg/ml penicillinstreptomycin-L-glutamine, and 10% FBS (Gibco Invitrogen, Carlsbad, CA) (van Zeeburg, et al. 2005). HEK293 and HeLa cells were cultured under the same conditions as VU1365. The subculture of OHSU974, VU1365 and HEK293 was conducted as described for the HNSCC cell lines.

3.2 GENERATION OF DNA DAMAGE

To induce DNA damage, the cells were continuously exposed to 80nM of mitomycin C (MMC) (Sigma, St. Louis, MO) for 24 hr for immunoblotting and quantitative reverse transcriptase PCR and 1 hr for focus formation.

3.3 FLUORESCENCE *IN SITU* HYBRIDIZATION

Fluorescence *in situ* hybridization (FISH) was performed to determine *FANCD2* gene copy number in HNSCC cell lines. The general FISH procedure was carried out as described earlier (Parikh, et al. 2007). To prepare mitotic cells for FISH analyses, HNSCC cells were harvested following a 5 hr treatment with 0.1 μg/ml Colcemid™ (Irvine Scientific, Santa Ana, California), hypotonic KCl (0.075 M) treatment for 16 min, and fixation in 3:1 methanol: glacial acetic acid. All other cells were harvested using the same method, except that 1 hr of Colcemid™ was preferred for nontumor cells. FISH analysis was used to detect copy number changes in the *FANCD2* gene in the HNSCC cell lines. For FISH analysis, cells were harvested, dropped onto slides, treated with 10 mg/ml RNase/2X SSC (0.6M NaCl, 0.06M Sodium Citrate, pH 7.0), and dehydrated using a graded series (70, 80, and 100%) of ethanol washes. Chromatin was denatured with 70% formamide and the cells were dehydrated in a second graded series of ethanol washes. The *FANCD2* probe for FISH was prepared following DNA extraction from BACs RP11-1022P15 and RP11-572M14 purchased from The Children's Hospital of Oakland Research Institute (CHORI, Oakland, CA). The BAC DNA was isolated using a BAC DNA miniprep procedure and labeled using a nick translation kit from Vysis/Abbott Molecular Inc. (Des Plaines, IL). The labeled DNA was precipitated with ethanol, resuspended in hybridization buffer, denatured for 5 min at 75°C, and preannealed for 15–30 min at 37°C. Each probe was hybridized for 16 hr at 37°C, after which slides were washed with 2X SSC/0.05% Tween-20. Slides were counterstained with 0.05 μg/ml 4',6-diamidino-2-phenylindole (DAPI) in 2X SSC and mounted with antifade (1,4-phenylene-diamine 1 mg/ml, in 86% glycerol/PBS, pH 8.0) (Sigma, St. Louis, MO) prior to analysis. All FISH analyses were carried out using an Olympus BX-61 epiflorescence microscope (Olympus Microscopes, Melville, NY). An Applied Imaging

CytoVision workstation with Genus v3.6 software was used for image capture and analysis (Applied Imaging, San Jose, CA).

3.4 RNA EXTRACTION AND QUANTITATIVE REVERSE TRANSCRIPTASE PCR

RNA was extracted by adding 1 ml of TRIzol® (Invitrogen, Carlsbad, CA) directly to the cells in the T25 flasks. TRIzol® was repeatedly pipetted over the cells to enhance cell lysis and produce a higher RNA yield. The tubes containing TRIzol and RNA mix were kept on ice prior to avoid RNA degradation. Then, 0.1 ml of 1-Bromo-3-chloropropane (BCP) (Sigma, St. Louis, MO) was added per 1ml of TRIzol into 2 ml microcentrifuge tubes. The mix was shaken vigorously by hand for 15 sec and incubated at room temperature (RT) for 3 min. The tubes were centrifuged for 15 min at 12,000 x g at 4°C. Following centrifugation, there were two layers. The upper aqueous layer containing RNA was transferred to a clean tube and mixed with 0.5 ml of isopropyl alcohol plus 1 µl of Glycogen (20µg/µl) for each ml of TRIzol® used. After incubation at RT for 10 min, the tubes were centrifuged at 12,000 x g at 4°C. After centrifugation, the RNA was in the pellet. The supernatant was removed and the pellet was washed one time with 70% Ethanol and centrifuged at 12,000 x g for 5 min at 4°C. After removing the supernatant, the RNA was slightly dried out (for about 5 min), but not dried completely. Then, the RNA pellets were resuspended in 100 µl of RNAse/DNAse free water and RNA purification was carried out using an RNeasy Mini Kit (Qiagen, Valencia, CA) according to the manufacturer's instructions. The RNA samples were cleaned of unwanted DNA using a DNA-free DNase Kit (Ambion, Foster City, CA) following the manufacturer's instructions. RNA concentrations were determined using the SmartSpec 3000 (Bio-Rad, Hercules, CA) and normalized to 40ng/ml. A good quality sample

had a 260/280 ratio of about 2.0 and a concentration of at least 40 µg/ml. Samples with ratios less than 1.6 and concentrations less than 30 µg/ml were re-extracted. The reverse transcription reaction was conducted with three inputs from each sample (400ng, 100ng and a negative control with no reverse transcriptase) for quality control. Universal Reference (UR) RNA (Stratagene, La Jolla, CA) was also included in the RT reaction at the same concentrations as the test samples. The reagents used in one reverse transcription reaction were as follows:

Table 1. Master Mix and Reverse Transcriptase reaction set-up.

Reagents	Company	Input		
		400ng	100ng	No Reverse Transcriptase (NRT)
10X PCR Buffer II	Applied Biosystems	10 µl	10 µl	10 µl
$MgCl_2$ (25mM)	Applied Biosystems	30 µl	30 µl	30 µl
dNTPs (25mM)	Roche Molecular Biochemicals	4 µl	4 µl	4 µl
MMLV (10U/µl)	Epicentre	1 µl	1 µl	0 µl
RNase Inhibitor (40U/µl)	Applied Biosystems	1 µl	1 µl	1 µl
Hex Primers (500 µM)	Applied Biosystems	2.5 µl	2.5 µl	2.5 µl
Nuclease-free water	Applied Biosystems	41.5 µl	49 µl	42.5 µl
Total		90 µl	97.5 µl	90 µl
RNA		10 µl	2.5 µl	10 µl

The ThermoCycler conditions were as follows: 25°C for 10 min, 48°C for 40 min, 95°C for 5 min and hold at 10°C. Later, the PCR products from the UR and test samples were diluted by 2.5 in nuclease-free water (100µl of cDNA + 150µl of nuclease-free water). The concentrations were then diluted to 160ng, 40ng and 160NRT.

TaqMan® primers and probes for FANCD2 (Hs00276992_m1), 18S (Hs99999901_s1), and universal reference RNA were purchased from Applied Biosystems (Applied Biosystems, Foster City, CA). Quantitative reverse transcriptase PCR (QPCR) was performed on the cDNA using the ABI 7700 Sequence detection instrument (Applied Biosystems) and analyzed using the

relative quantitation method (User Bulletin, PE Applied Biosystems) as in (Huang, et al. 2002). For the QPCR, 2X TaqMan Buffer was prepared to make either a final volume of 1ml or 5ml, depending on the number of samples to be analyzed, as follows:

Table 2. Master Mix for 2X TaqMan Buffer set-up.

Reagents	Company	Final volume of 1ml	Final volume of 5ml
10X Buffer A	Applied Biosystems	200 µl	1 ml
Nuclease-free water	Applied Biosystems	486 µl	2.43 ml
dNTPs (25mM)	Roche Molecular Biochemicals	24 µl	120 µl
$MgCl_2$ (25mM)	Applied Biosystems	280 µl	1.4 ml
Amplitaq Gold® DNA Polymerase	Applied Biosystems	10 µl	50 µl

The reagents used to set-up one QPCR reaction were as follows:

Table 3. Master Mix for QPCR set-up.

Reagents	Company	Volume
2X TaqMan Buffer	Self-made in our laboratory	10 µl
Primers [reverse and forward (5µM) each] and probe (105µM) stock concentrate mix	Applied Biosystems	1 µl
Nuclease-free water	Applied Biosystems	7 µl
cDNA		2 µl

The ThermoCycler conditions for the QPCR were 95°C for 12 min for one cycle and 40 cycles of 95°C for 15 sec followed by 63°C for 60 sec. Each sample was run in triplicate along with the no reverse transcriptase control. No template controls were also set-up for each plate consisting of QPCR master mix but without cDNA. The RNA levels were quantified relative to the Universal Reference RNA.

3.5 IMMUNOBLOTTING

To evaluate FANCD2 protein monoubiquitination, we prepared total protein lysates from HNSCC cell lines as described previously (Garcia-Higuera, et al. 2001; Parikh, et al. 2007) with some modifications. Flasks of cells were trypsinized and washed in ice cold 1X PBS and lysed in 2X lysis buffer containing 100 mM Tris-HCl (pH 6.8), 12% 2-mercaptoethanol, 4% sodium dodecyl sulfate (SDS), 1mM dithiothreitol (DTT), 10 µg/ml of leupeptin, 10 µg/ml pepstatin and 1nM of phenyl methyl sulfonyl fluoride (PMSF). The cell lysates were boiled for 5 min. Protein concentrations were determined using the Bio-Rad RC DC Protein Assay Kit, due to the high concentration of detergent like SDS and reducing agents like DTT and 2-mercaptoethanol. The SmartSpec 3000 (Bio-Rad, Hercules, CA) was used for the photometric readings of protein concentrations. Cell lysates were normalized to 1 µg/ml. 20 to 30 µl of the samples were run by Tris-HCl polyacrylamide gradient gels electrophoresis of 6% and 12%. Also, 10 µl of Precision Plus Protein standards were loaded in the gel to keep track of the running bands. The gels were run at 75 V for 25 min and later increased to 135 V until the bands reached the lower bottom of the gel in approximately 1 hr and 30 min. Later, the proteins were transferred to Hybond N+ nylon membrane (Amersham Biosciences, Piscataway, NJ) at 135 V for 1 hr and 30 min. During the transfer, the electrophoresis chamber was kept submerged in ice all the time to avoid the destruction of the membrane due to the excessive heat generated from the high voltage. Membranes were blocked in 5% non-fat dry milk in 1X PBS with 0.1% Tween-20 (TPBS) for 1 hr at RT. Membranes were incubated with mouse monoclonal anti-FANCD2 FI17 (Santa Cruz Biotechnology, Santa Cruz, CA) antibody at 1:1000 dilutions in 0.5% BSA/TPBS) overnight at 4ºC, followed by incubation with either HRP-conjugated goat anti-mouse IgG at a 1:5000 dilution or HRP-conjugated goat anti-rabbit IgG at a 1:2,500 dilution both in 5% non-fat dry

milk in 1X PBS with 0.1% Tween-20. Other antibodies used were rabbit polyclonal anti-TP53 at a 1:1000 dilution, rabbit polyclonal anti-phospho-TP53 at a 1:100 dilution, rabbit polyclonal anti-FHIT at a 1:5000 dilution and, mouse monoclonal anti-RAD9 at a 1.5 μg/ml dilution. The proteins were visualized using the Western Lighting™ Chemiluminescence Reagent (Perkin Elmer, Boston, MA) according to the manufacturer's instructions. To verify equal protein loading in the gels, membranes were cut and probed with antibodies against proteins from housekeeping genes like β-actin (Abcam, Cambridge, MA) at a 1,5000 dilution and α-actinin (Santa Cruz Biotechnology) at a 1:5000 dilution in 0.5% BSA/TPBS. Antibodies against β-actin were used when the expected band of the protein of interest was larger than 60 kDa. Antibodies against α-actinin were used when the expected band of the protein of interest was lower than 60 kDa. As far as FANCD2, in untreated cells we expected to see a band at 155kDa, the non-monoubiquitinated form of FANCD2, also known as the short form (FANCD2-S). After treatment of the cells with MMC, we expected to see an additional band that ran a little higher (162 kDa) because of the addition of the ubiquitin to FANCD2. This band is also known as the long form (FANCD2-L). The FANCD2-L/FANCD2-S ratio was determined by a densitometric analysis using Un-Scan-It Gel™ (Silk Scientific, Orem, UT). This program is able to determine the intensity of the bands from a western blot by measuring the number of pixels from each band, therefore, providing a numerical value for each band observed in the gel. The expected MW of the bands from the proteins studied were as follows: 53 kDa for total TP53, 53 kDa for phospho-TP53, 17 kDa for FHIT, and 50 kDa for RAD9.

3.6 IMMUNOFLUORESCENCE MICROSCOPY

FANCD2 focus formation was tested after exposing HNSCC to 80nM MMC. The cell lines were passaged into single-well chamber slides one day prior the treatment with MMC. A parallel set of chamber slides was also prepared as a normal control (culture medium only). After treatment, the wells were washed with 1X Hanks' Balanced Salt Solution (HBSS) (Irvine Scientific), fresh medium was added and the cells were returned to incubate for 3 hr to allow for DNA repair. After repair, cells were washed with 1X PBS, fixed in 4% paraformaldehyde (PFA) in 1X PBS for 20 min and permeabilized with 0.5% Triton-X (Sigma) in 1X PBS for 10 min. After permeabilization, cells were blocked with 5% Bovine Serum Albumin (BSA) (Sigma) in 0.2% Tween-20/PBS for 30 min. Then, cells were incubated with affinity-purified E35 rabbit polyclonal anti-FANCD2 antibody at a 1:200 dilution and mouse monoclonal anti-RAD51 at a dilution of 1:500 both in blocking buffer for 2 hr at room temperature. After washing three times for 5 min each with 0.2% Tween-20/PBS, cells were then incubated with both anti-rabbit FITC-conjugated antibody at 15µg/ml and anti-mouse TRITC-conjugated antibody at 15µg/ml in blocking buffer for 1 hr at room temperature. Then, after washing three times for 5 min each with 0.2% Tween-20/PBS, cells were counterstained with 0.05 µg/ml 4',6-diamidino-2-phenylindole (DAPI) in 2X SSC for 2 min and mounted using antifade (1,4-phenylene-diamine 1 mg/ml, in 86% glycerol/PBS, pH 8.0) (Sigma, St. Louis, MO)) (Hussain, et al. 2004). The number of cells showing FANCD2 and RAD51 focus formation were scored by using an Olympus BX-61 epiflorescence microscope (Olympus Microscopes, Melville, NY). An Applied Imaging CytoVision workstation with Genus v3.6 software was used for image capture and analysis (Applied Imaging, San Jose, CA). A total of 100 cells were scored from control and MMC-treated chamber slides for each of the cell lines.

3.7 PREPARATION AND USE OF THE CHEK1 SMALL MOLECULE INHIBITOR (SMI)

Initially, the CHEK1 SMI was provided in powder form and 10mM stock solution was prepared in 100% DMSO (stock solution) by using the compound's formula weight. Then, 1 ml of 1 mM CHEK1 SMI working solution was prepared by diluting 100 µl of 10 mM CHEK1 SMI stock solution in 900 µl of 100% DMSO. Finally, the 1 mM working solution previously prepared was used to prepare the different concentrations of CHEK1 SMI (180 nM, 360 nM and 540 nM) by diluting 1 mM CHEK1 SMI working solution directly in fresh medium. The amount of medium containing CHEK1 SMI to be used depended on how many plates were going to be treated. To preserve the compound stability, it was kept protected from the light at room temperature according to manufacturer's instructions.

3.8 CLONOGENIC SURVIVAL ASSAY

To determine the effect of the CHEK1 SMI on cell survival, HNSCC cell lines were tested when 70 to 80% confluency was reached to ensure that cells were actively dividing. After washing the cells once with 1X Hanks' Balanced Salt Solution (HBSS) (Irvine Scientific), 0.05% trypsin-0.02%EDTA (Gibco Invitrogen) was added to the flasks and were incubated for 2 to 5 min at 37°C in 5% CO_2 humidified incubator. To ease the detachment of the cells, the flasks were taken

out of the incubator and tapped a couple of times. Prolonged exposure of the cells (more than 5 min) to trypsin was avoided to reduce cellular stress. M10 medium was added to the flask at a volume of twice of the volume of trypsin to inactivate the trypsin. The cells and the medium were placed in a 15 ml conical tube and centrifuged at 600 x g for 6 min. The supernatant was discarded and cells were resuspended in 1 to 2 ml of media depending on the size of the pellet. Cells were mixed and 20 µl of the suspension were mixed with 20µl of 0.5% of Trypan Blue/saline solution in a separate tube. Then, 10µl of the mix were placed in a hemacytometer for cell counting. For the clonogenic survival assay, 2 x 10^3 cells were plated in triplicate in 60 mm Petri dishes. Cells were allowed to attach for 24 hr prior treatment with IR. Then, the cells were treated with increasing doses of IR at 0, 2.5, 5.0 and 10.0 Gy and were simultaneously treated with increasing doses of CHEK1 SMI for 24 hr immediately after IR treatment. Following the manufacturer's recommendations, we used 4X (180nM), 8X (360nM) and 12X (540nM) of the CHEK1 SMI EC_{50} (45nM). As a control, the cells were untreated with IR. Also, as a CHEK1 SMI control the cells were exposed to DMSO only, which was used to dilute the CHEK1 SMI. Medium was changed 24 hr after treatment with fresh medium without SMI and changed again at day 7. After 12 days of incubation the medium was removed from the cell colonies and they were fixed with 70% ethanol for 5 min. Then, the ethanol was discarded and 10% Giemsa (Sigma) in water was added to the plates for 5 min to stain the cell colonies. Later, the plates were washed with tap water to eliminate the Giemsa. The plates were dried on the bench overnight. Prior to counting, a grid was drawn on the bottom of the plates to facilitate cell colony counting. The colony counting was conducted under a dissecting microscope (Olympus). A colony was considered as such if comprised of at least 50 cells. Experiments were performed

in triplicate and error was calculated as one standard deviation from the mean (Franken, et al. 2006; Parikh, et al. 2007).

3.9 FLOW CYTOMETRY

To assess the effect of the CHEK1 SMI on the cell cycle, we conducted a cell cycle analysis with propidium iodide (PI) staining by flow cytometry. For this procedure, 5 x 10^5 cells were fixed in 70% ethanol and stored at -20°C in 1.5 ml centrifuge tubes. The day of the analysis, the cells were centrifuged at 200 x g for 5 min, the supernatant was removed, and the cells were washed twice in 1X PBS. After the washes, the pelleted cells were suspended in 500 µl of 50 µg/ml Propidium Iodide with 10 µg/ml RNAse A solution in 1X PBS. After an incubation of 30 min, the cells were taken to the University of Pittsburgh Cancer Institute Flow Cytometry lab and analyzed in a Dako CyAn ADP (DAKO) flow cytometer (Darzynkiewicz and Juan 2001). At least 50,000 cells per sample were analyzed by the equipment. The results were further analyzed using the software ModFit LT (Verity Software house, Topsham, ME). Based on DNA content alone, this software uses a mathematical model called deconvolution to discern the three cell cycle populations G_0/G_1, S, and G_2/M. In this way, we were able to determine any change in the cell cycle populations after exposure of HNSCC cell lines to CHEK1 SMI and IR.

4.0 RESULTS

4.1 CELL LINE DESCRIPTION

This study was conducted on fourteen HNSCC cell lines originally generated in the laboratory of Dr. Susanne M. Gollin (White, et al. 2007), two HNSCC cell lines derived from FA patients, HeLa and HEK293 cells.

Table 4. Characteristics of the patients and cell lines used in the study.

Cell line	Smoking/ alcohol history[1]	Family history of HNSCC[1]	3ploss[2]	Ploidy[2]	Ethnicity	HPV[1]
UPCI:SCC029B	+/+	-	-	3	Caucasian	-
UPCI:SCC032	+/+	+	+	2	Caucasian	-
UPCI:SCC040	-/+	+	-	3	Caucasian	-
UPCI:SCC066	+/+	+	-	4	Caucasian	-
UPCI:SCC070	+/+	+	+	3	Caucasian	-
UPCI:SCC078	-/+	+	+	3-4	Caucasian	-
UPCI:SCC084	+/+	-	+	2	Caucasian	-
UPCI:SCC099	+/+	+	-	2-4	Caucasian	+
UPCI:SCC103	+/-	-	+	5	Caucasian	-
UPCI:SCC104	+/+	-	+	4-5	Caucasian	-
UPCI:SCC105	+/+	+	-	3	Caucasian	-
UPCI:SCC116	+/+	+	+	3-4	Caucasian	-
UPCI:SCC131	+/+	-	-	4	Caucasian	-
UPCI:SCC142	+/+	U	-	3	Caucasian	-
OHSU974	U	U	U	3	Caucasian	-
VU1365	U	U	U	3	Caucasian	-
HeLa	U	U	U	4	Caucasian	-

"U" refers to Unknown. The data were obtained from White[1] and Martin[2] (Martin, et al. 2008; White, et al. 2007).

As depicted in Table 4, previous studies in our laboratory have already shown that around 85% of the HNSCC cell lines studied here come from patients with a positive smoking and drinking history.

Fifty percent of the HNSCC cell lines from patients with a smoking and alcohol history showed loss of the short arm of chromosome 3 (3p). This is consistent with the observation that 3p loss is a common and early observation, not only in head and neck cancer (Tsui, et al. 2008), but also in breast (Maitra, et al. 2001), lung (Todd, et al. 1997), and ovarian cancer (Todd, et al. 1997), among others. Therefore, it is reasonable to investigate the effects of 3p loss in HNSCC cell lines.

4.2 DECREASED FHIT PROTEIN EXPRESSION IN HNSCC CELL LINES

Previous studies have shown the presence of aberrant *FHIT* gene expression in our HNSCC cell lines suggesting breakage at chromosome band 3p14.2, which encompass the fragile site FRA3B (Virgilio, et al. 1996). HEK293 cells, which have been suggested to have a potential neuronal origin (Shaw, et al. 2002), were used as a positive control because it has been observed that endogenous FHIT protein is strongly expressed by these adenovirus 5 T-antigen-transformed cells (Druck, et al. 1997; Ishii, et al. 2006). A rabbit anti-FHIT polyclonal antibody that recognizes the entire 17 kDa FHIT protein (Druck, et al. 1997) was used to detect endogenous levels of FHIT protein expression in the HNSCC cell lines. As shown in Figure 3, we observed that FHIT protein expression was downregulated in twelve of the fourteen HNSCC cell lines, including UPCI:SCC032, 040, 066, 084, 099, 103, 105, 116, 131, 142 and 029B. Nine of the

twelve FHIT protein-deficient HNSCC cell lines came from patients with smoking history. Only UPCI:SCC040 and 142 came from patients without a smoking history (or with an unknown smoking history). Decreased FHIT protein expression was also observed in OHSU974 and VU1365 cell lines (HNSCC cell lines derived from FA patients). Only UPCI:SCC078 and 104 showed FHIT bands with reduced intensity compared to the FHIT-positive control, HEK293. It is worth noting that UPCI:SCC078 comes from a patient who had an alcohol consumption history only, while UPCI:SCC104 comes from a patient with both a history of smoking and alcohol consumption. Considering that the fragile site FRA3B encompasses the *FHIT* gene and that reduced *FHIT* gene and protein expression have been observed in cells without activated FRA3B, particularly in cancer cells from patients with a smoking history (Stein, et al. 2002), our results are consistent with previous observations.

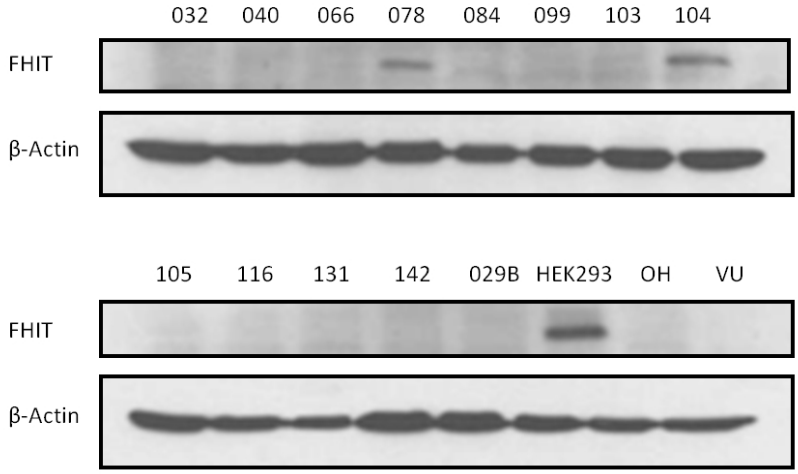

Figure 3. FHIT protein expression in HNSCC cell lines.

FHIT protein expression was evaluated in fourteen UPCI:SCC HNSCC cell lines by western blotting. Decreased FHIT protein expression was observed in 11 HNSCC cell lines. Only two HNSCC cell lines, UPCI:SCC078 and 104 show the expected band for the FHIT protein (17 kDa). Two HNSCC cell lines, OHSU973 and VU1365 derived from FANCA $^{-/-}$ patients also showed decreased FHIT protein expression. HEK293 was used as positive control.

4.3 *FANCD2* GENE COPY NUMBER LOSS IN HNSCC CELL LINES

We next investigated whether there is a correlation between decreased FHIT expression and *FANCD2* gene copy number. For this purpose, FISH was conducted in fourteen UPCI:SCC cell lines and two FA-derived HNSCC cell lines to determine the of *FANCD2* gene copy number status. *FANCD2* gene copy number was determined by using a BAC probe to *FANCD2,* labeled with SpectrumGreen™ relative to the number of chromosome 3 centromeres in each cell line, marked using the CEP3 probe labeled with SpectrumOrange™. We observed that eleven of the fourteen cell lines evaluated (UPCI:SCC029, 032, 040, 070, 078, 084, 099, 104, 105, 116, 131, and 142) showed relative *FANCD2* gene copy number loss (Figures 4 and 5). HNSCC cell lines, OHSU974 and VU1465 also showed *FANCD2* gene copy number loss. Contrary to this observation UPCI:SCC066 and 131 did not show *FANCD2* gene copy number loss. HeLa cells were used as a FA/BRCA pathway proficient control and they did not show FANCD2 gene copy number loss. Ideally, a normal cell lines is used as control but since OKF6/TERT-1 show decrease FANCD2 protein and gene expression we decided to use a proficient FA/BRCA pathway cell line even though it is a cancer cell. Thus, HNSCC cell lines that exhibited decreased FHIT protein expression also showed *FANCD2* gene copy loss. The only exceptions were UPCI:SCC078 and 104, which showed FHIT protein expression and *FANCD2* gene copy number loss. Another interesting observation was that UPCI:SCC066 and 103 did not show *FANCD2* gene copy number loss but they showed decreased FHIT protein expression.

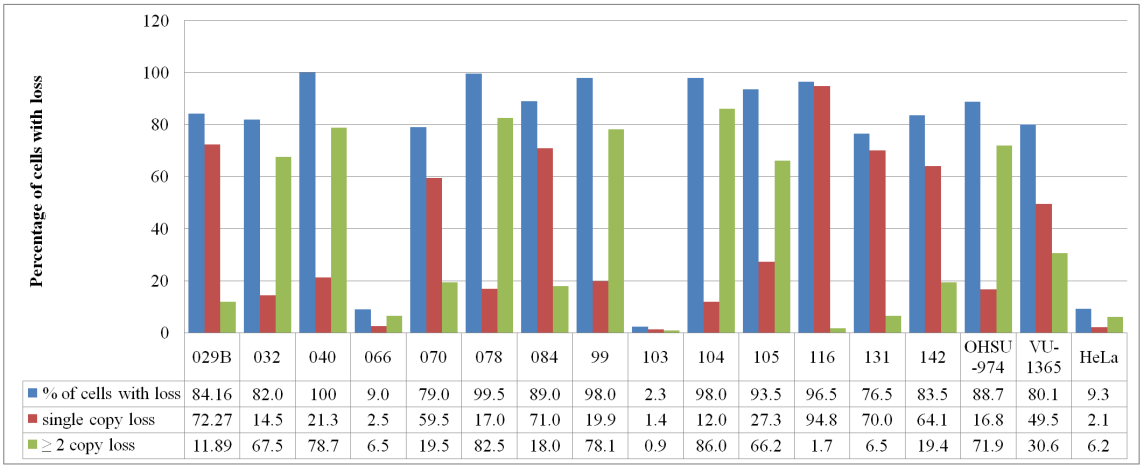

	029B	032	040	066	070	078	084	99	103	104	105	116	131	142	OHSU-974	VU-1365	HeLa
% of cells with loss	84.16	82.0	100	9.0	79.0	99.5	89.0	98.0	2.3	98.0	93.5	96.5	76.5	83.5	88.7	80.1	9.3
single copy loss	72.27	14.5	21.3	2.5	59.5	17.0	71.0	19.9	1.4	12.0	27.3	94.8	70.0	64.1	16.8	49.5	2.1
≥ 2 copy loss	11.89	67.5	78.7	6.5	19.5	82.5	18.0	78.1	0.9	86.0	66.2	1.7	6.5	19.4	71.9	30.6	6.2

Figure 4. Loss of *FANCD2* gene copy number in fourteen HNSCC cell lines determined by FISH

Percentage of cells showing *FANCD2* gene copy number loss by FISH. The blue bars indicate the percentage of cells with relative loss compared to CEP3. Red bars indicate percentage of cells with single copy loss and green bars indicate percentage of cells with loss of more than 2 copies.

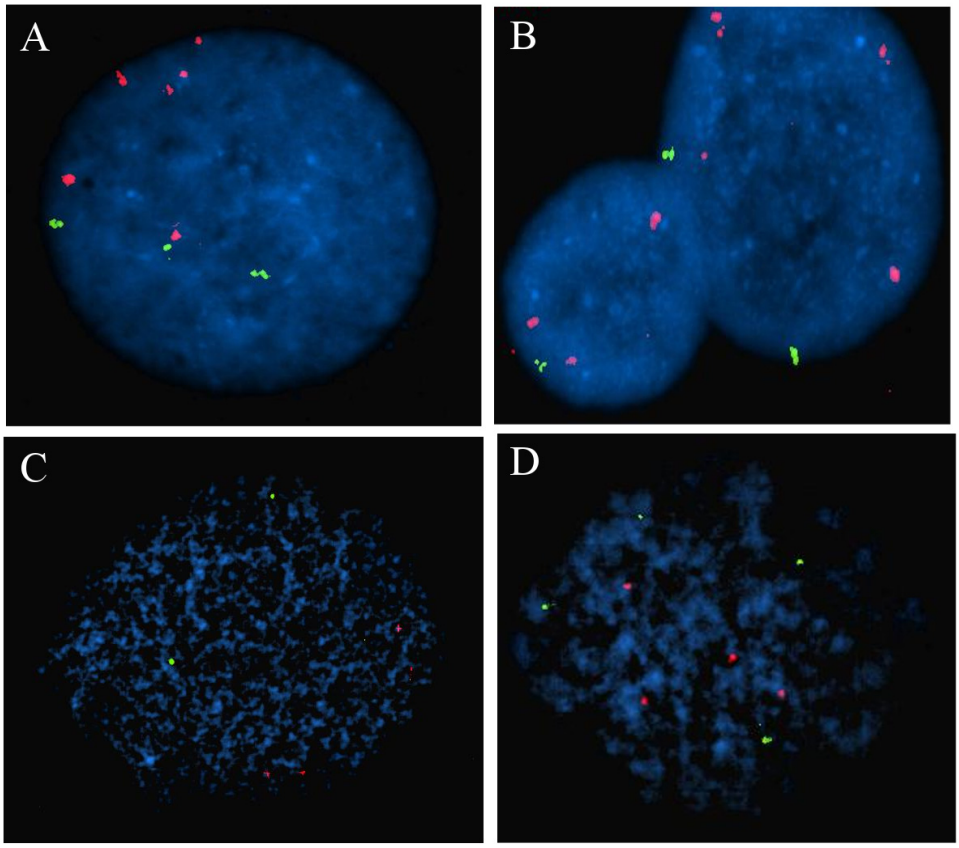

Figure 5. FISH results for *FANCD2* compared to CEP3

FISH using BAC probes mapping to *FANCD2,* labeled with SpectrumGreen™ (green signal) and CEP3 labeled with SpectrumOrange™ (orange signal) demonstrates that *FANCD2* is lost in HNSCC cell lines **(A)** UPCI:SCC104, **(B)** UPCI:SCC070, and **(C)** HNSCC cell line OHSU974, derived from a FA patient. **(D)** HeLa cells showed no FANCD2 loss.

4.4 INDUCTION OF *FANCD2* GENE EXPRESSION IN RESPONSE TO MMC IS DECREASED IN HNSCC CELL LINES

To determine if loss of *FANCD2* gene copy number influences gene expression, HNSCC cell lines were exposed to 80 ng/ml MMC for 24 hr. RNA was extracted for QPCR. As negative

controls, we included OHSU-974 and VU-1365 which are HNSCC cell lines derived from FA patients. They were considered to be good negative controls because they have a mutated *FANCA* gene, part of the FA core complex. Therefore, upon exposure to MMC, the FA core complex integrity is compromised, failing to assemble at the DNA damage site. This eventually leads to defective FANCD2 monoubiquitination and DNA damage repair. We also included HeLa as a FA/BRCA pathway proficient cell line. The hTERT transfected keratinocytes, OKF6/TERT-1, were not used as a normal control because they have decreased FANCD2 gene and protein expression (Dr. Toshiyasu Taniguchi, personal communication). When untreated with MMC, we observed 1 to 3-fold decrease *FANCD2* baseline expression in seven of the fourteen HNSCC cell lines (UPCI:SCC070, 084, 099, 104, 116, 131, and 142) compared to the FA/BRCA proficient HeLa cell line (Figure 6, blue bars). The same observation was made in the HNSCC cell lines derived from FA patients, OSHU974 and VU1365. On the contrary, HNSCC cell lines (UPCI:SCC029B, 032, 066, 078, 105, and 131) showed baseline *FANCD2* gene expression similar to or higher than the FA/BRCA proficient HeLa cell line.

We also observed 1.5 to 2.5-fold decreased induction of *FANCD2* gene expression upon exposure to MMC in all the HNSCC cell lines, including the HNSCC derived from FA patients (Figure 6, red bars and Figure 7). On the contrary, only two of the fourteen cell lines (UPCI:SCC040 and UPCI:SCC103) exhibited similar or higher induction of the *FANCD2* gene expression.

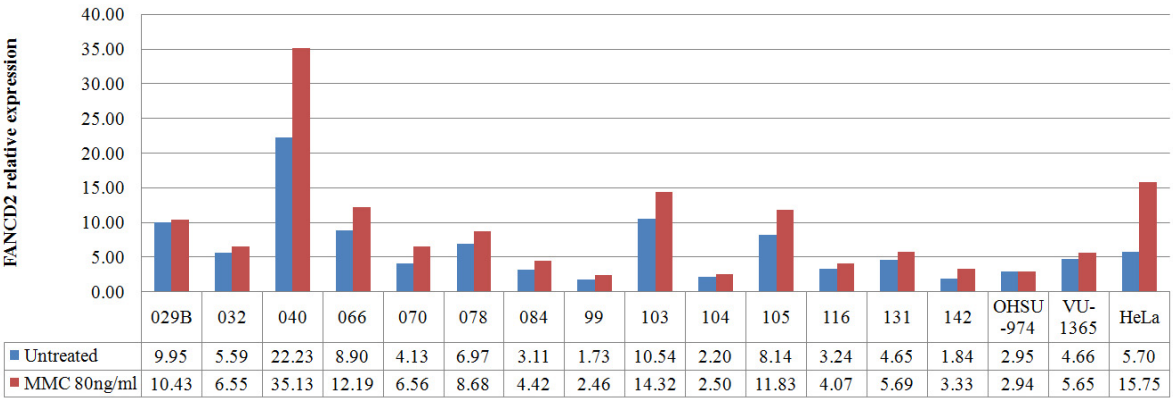

	029B	032	040	066	070	078	084	99	103	104	105	116	131	142	OHSU-974	VU-1365	HeLa
Untreated	9.95	5.59	22.23	8.90	4.13	6.97	3.11	1.73	10.54	2.20	8.14	3.24	4.65	1.84	2.95	4.66	5.70
MMC 80ng/ml	10.43	6.55	35.13	12.19	6.56	8.68	4.42	2.46	14.32	2.50	11.83	4.07	5.69	3.33	2.94	5.65	15.75

Figure 6. FANCD2 baseline and induced expression in HNSCC cell lines with and without exposure to MMC.

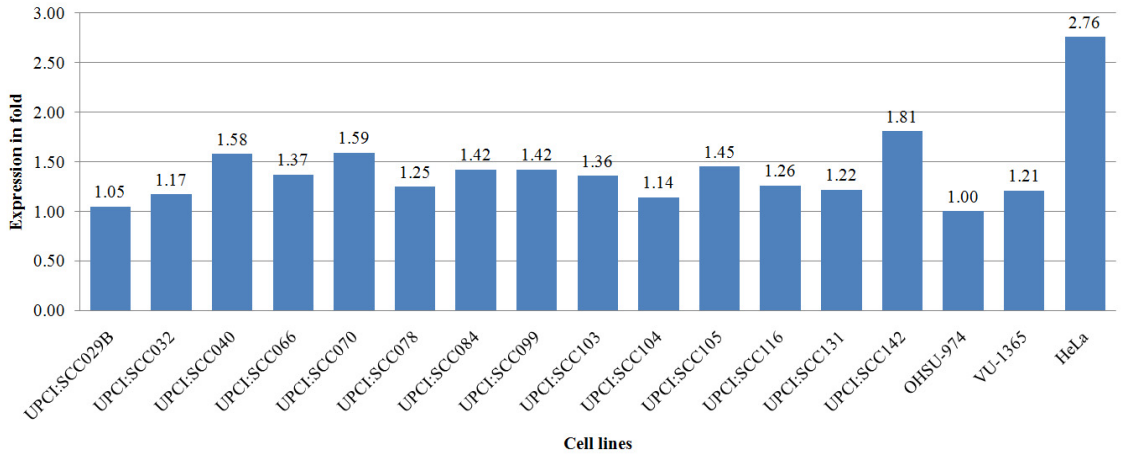

Figure 7. Induced *FANCD2* gene expression in HNSCC cell lines upon exposure to 80 ng/ml MMC.

4.5 FANCD2 PROTEIN EXPRESSION IS DECREASED IN HNSCC CELL LINES

To determine FANCD2 protein expression, western blotting was performed on lysates derived from HNSCC cell lines exposed to 80 ng/ml for 24 hr. When cells are not exposed to MMC FANCD2 is seen as a band of 155 kDa called short form (S) or faster migrating. After the cells

are exposed to MMC, FA pathway activation leads to the formation of the core complex and FANCD2 monoubiquitination. The latter is observed as a shift in the migration of the 155 kDa band to a higher migrating band of 165 kDa called the long form (L) or slower migrating band, resulting in a pattern of double bands. Therefore, the lower band is the non-monoubiquitinated FANCD2 (Short form, S) and the upper band is the monoubiquitinated FANCD2 (Long form, L). A ratio of the L/S forms is used as an indicator of the level of FANCD2 monoubiquitination. We observed that 11 of the 14 HNSCC cell lines showed decreased overall FANCD2 protein expression that ranged from mildly (UPCI:SCC084, 104, and 142) to moderately decreased (UPCI:SCC029B, 066, 099, 103, 032, 078, 105, and 131) compared to the FA/BRCA proficient HeLa cell line (Figure 8). Only three HNSCC cell lines (UPCI:SCC040, 070 and 116) exhibited FANCD2 protein expression similar to the FA/BRCA proficient HeLa cell line.

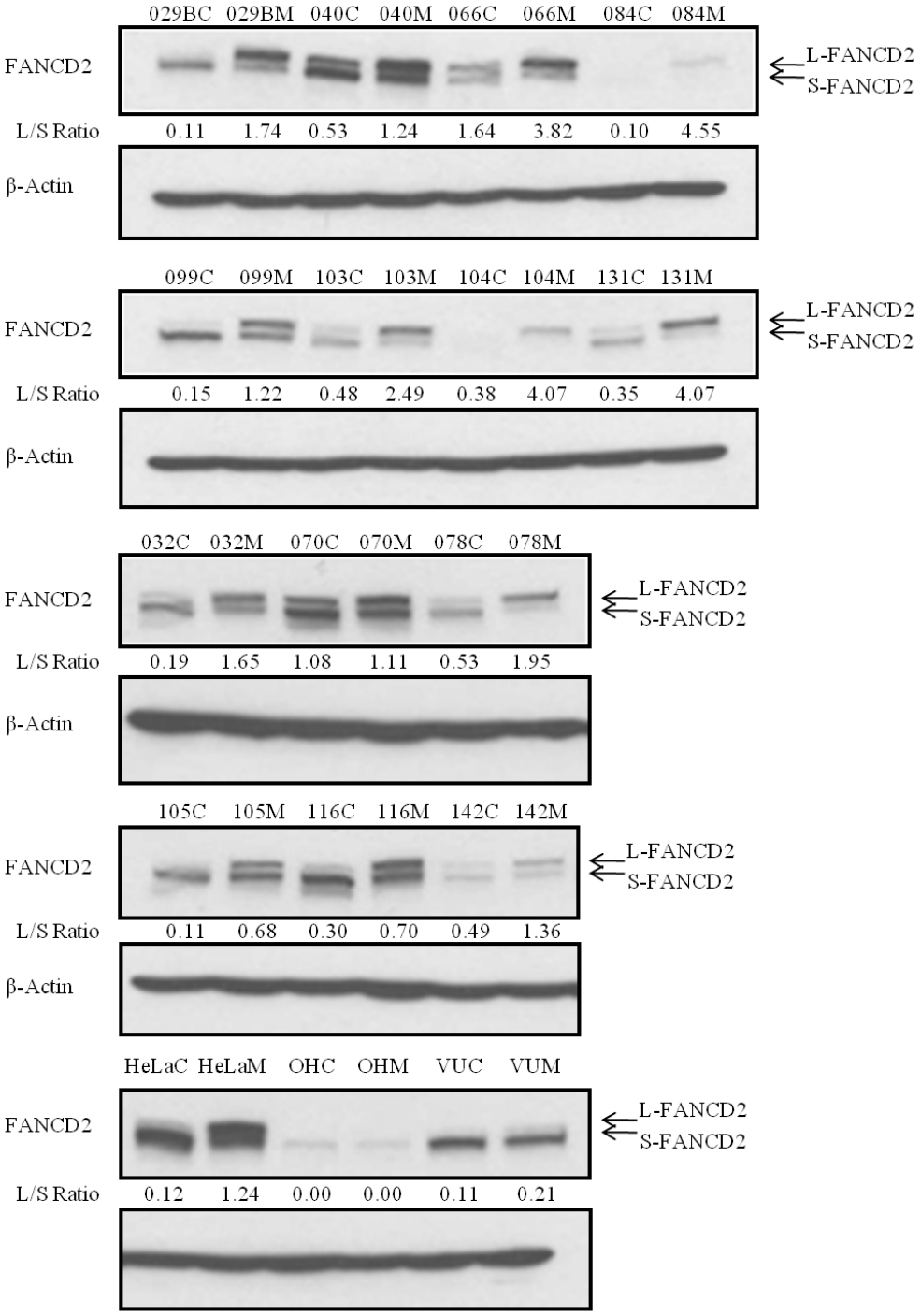

Figure 8. FANCD2 western blot of HNSCC cell lines.

FANCD2 protein expression was evaluated in 14 HNSCC cell lines including the HNSCC cell lines derived from FA patients, OHSU974 (OH) and VU1365 (VU) and the FA/BRCA pathway proficient cell line (HeLa).

The induction of the FANCD2 monoubiquitinated form (L) was also assessed in HNSCC cell lines upon exposure to 80 ng/ml of MMC for 24 hr. By comparing the L/S ratio of the HNSCC cell lines to the FA/BRCA proficient cell line, we observed that only two HNSCC cell lines showed 0.5-fold decreased induction [UPCI:SCC105 (L/S Ratio: 0.68) and UPCISCC116 (L/S Ratio: 0.70)] compared to the FA/BRCA proficient cell line [HeLa (L/S Ratio: 1.24)]. The remaining 12 HNSCC cell lines showed an equal or higher induction ratio [UPCI:SCC029B (L/S Ratio: 1.74), UPCI:SCC040 (L/S Ratio: 1.24), UPCI:SCC066 (L/S Ratio: 3.82), UPCI:SCC084 (L/S Ratio: 4.55), UPCI:SCC099 (L/S Ratio: 1.22), UPCI:SCC103 (L/S Ratio: 2.49), UPCI:SCC104 (L/S Ratio: 4.07), UPCI:SCC131 (L/S Ratio: 4.07), UPCI:SCC032 (L/S Ratio: 1.65), UPCI:SCC070 (L/S Ratio: 1.11), UPCI:SCC078 (L/S Ratio: 1.95), and UPCI:SCC142 (L/S Ratio: 1.36)] compared to the FA/BRCA proficient cell line (Figure 8). HNSCC cell lines derived from FA patients were also included in the study and they show both displayed decreased overall FANCD2 protein expression and decreased induction of the monoubiquitinated form (L) with and without treatment with MMC [OHSU974 (L/S Ratio: 0.00) and VU1365 L/S Ratio: 0.21)].

4.6 DECREASED FANCD2 AND RAD51 FOCUS FORMATION IN HNSCC CELL LINES

To determine the functionality of the FA/BRCA pathway and its effect on DNA damage repair through the activation of homologous recombination repair (HR), we evaluated the ability of the HNSCC cell lines to form FANCD2 and RAD51 foci, respectively. Specific antibodies against FANCD2 and RAD51 were used in a co-staining procedure. FANCD2 and RAD51 foci were counted in parallel by changing the filters in the same microscopic field. We observed that untreated HNSCC cell lines exhibited endogenous FANCD2 and RAD51 focus formation ranging from 11% to 49% of focus positive cells (Figure 9, 10, 11 and 12). No endogenous FANCD2 focus formation was observed in HNSCC cell lines derived from FA patients (OHSU974 and VU1365) as depicted in Figure 13. HNSCC cell lines derived from FA patients (OHSU974 and VU1365) only showed a scattered staining for FANCD2 and RAD51. The untreated FA/BRCA proficient cell lines showed endogenous FANCD2 and RAD51 foci formation as 24% of cells expressed foci (Figure 9 and 10) as depicted in Figure 14. After exposure to MMC, HNSCC cell lines showed induction of FANCD2 and RAD51 focus formation in a lower percentage of cells compared to the FA/BRCA proficient cell line, ranging from 35% to 89% of cells with foci (Figures 9 and 10). Only UPCI:SCC040, 103 and 104 showed higher frequency of FANCD2 and RAD51 foci formation among HNSCC cell lines from the general population. Even though HNSCC cell lines derived from FA patients did not show either FANCD2 or RAD51 focus formation, they still showed a scattered staining for FANCD2 and RAD51. This indicates the inability of OHSU974 and VU1365 to form FANCD2 and RAD51 foci. After exposure to MMC, the FA/BRCA proficient cell lines showed increased FANCD2 and RAD51 focus formation in 98% of the cells. Figures 9 and 10 also shows that after

exposure to MMC, some of cells comprising the HNSCC cell population did show FANCD2 and RAD51 focus formation while others did not. This was not observed in the FA/BRCA proficient HeLa cell line, which showed FANCD2 and RAD51 focus formation in all of the cells under the same conditions. These results show that the HNSCC under study have a limited ability to induce both FANCD2 and RAD51 foci upon exposure to MMC.

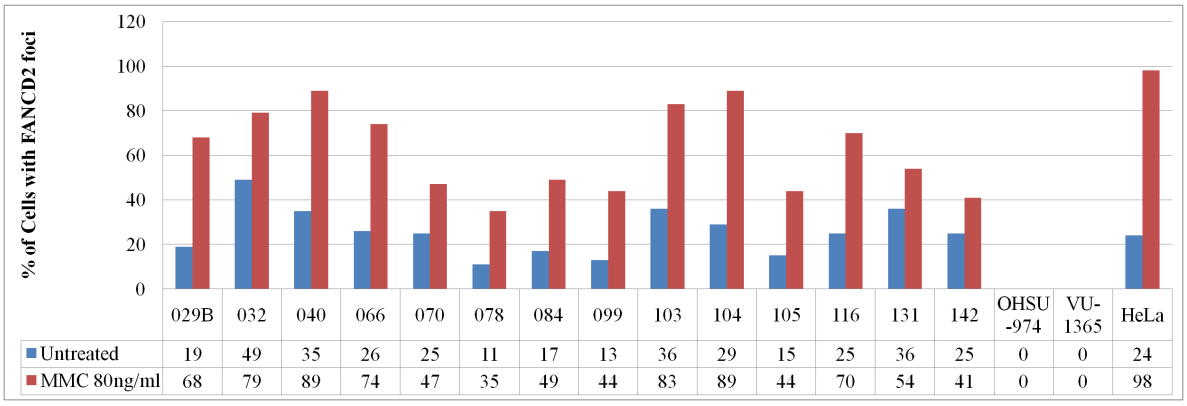

Figure 9. Bar graph showing the percentage of HNSCC cells with FANCD2 foci.

The distribution of FANCD2 foci was assessed in HNSCC cell lines from the general population, HNSCC cell lines derived from FA patients (OHSU974 and VU1365), and a FA/BRCA proficient cell line (HeLa) treated and untreated with MMC for 24 hr.

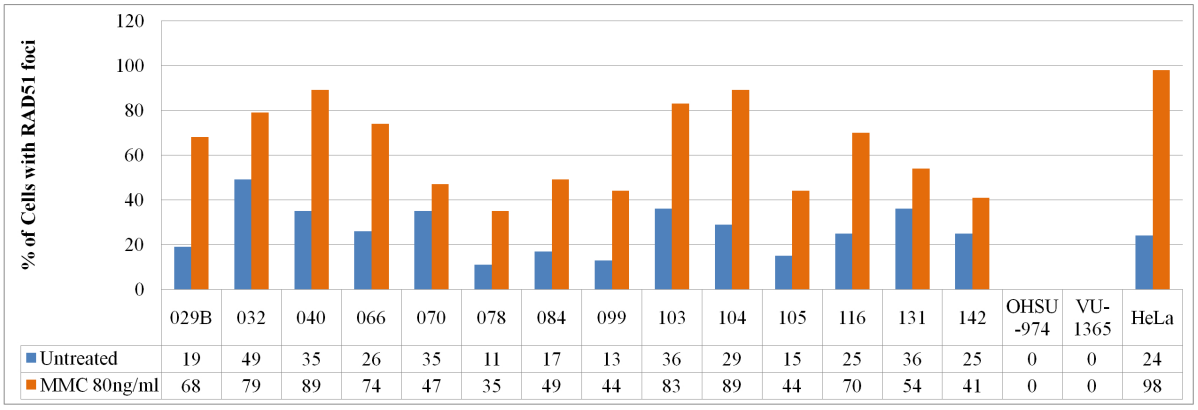

Figure 10. Bar graph showing the percentage of HNSCC cells with RAD51 foci.

The bar graph shows the distribution of RAD51 foci in HNSCC cell lines derived from patients from the general population, HNSCC cell lines derived from FA patients (OHSU974 and

VU1365), and a FA/BRCA proficient cell line (HeLa) treated and untreated with MMC for 24 hr. FANCD2 and RAD51 foci were counted in the same cells by changing the filters in the same microscopic field.

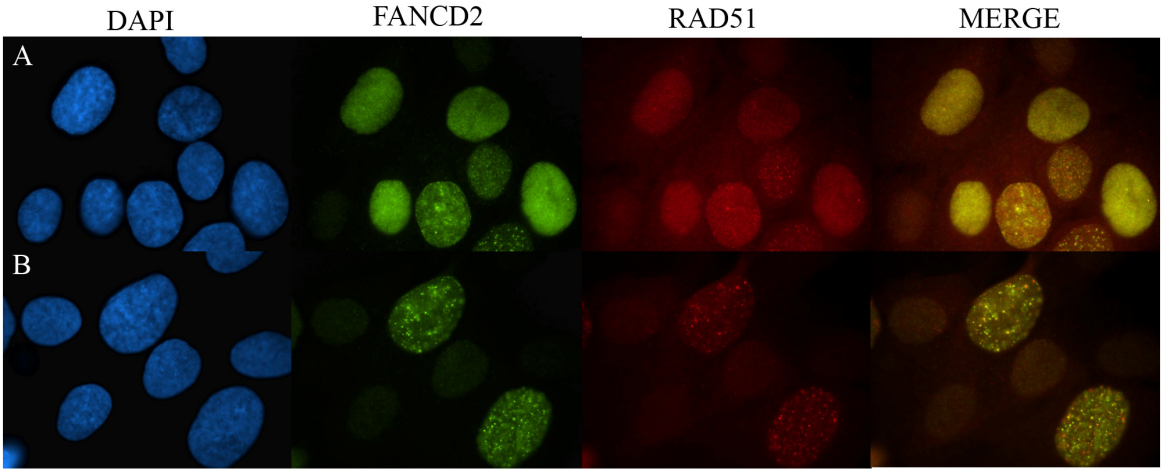

Figure 11. UPCI:SCC131 showing decreased FANCD2 and RAD51 focus formation.

Decreased FANCD2 and RAD51 focus formation in UPCI:SCC131 with and without exposure to 80 ng/ml of MMC for 24 hr. **(A)** Untreated cells; **(B)** cells treated with 80 ng/ml of MMC showed decreased FANCD2 and RAD51 foci.

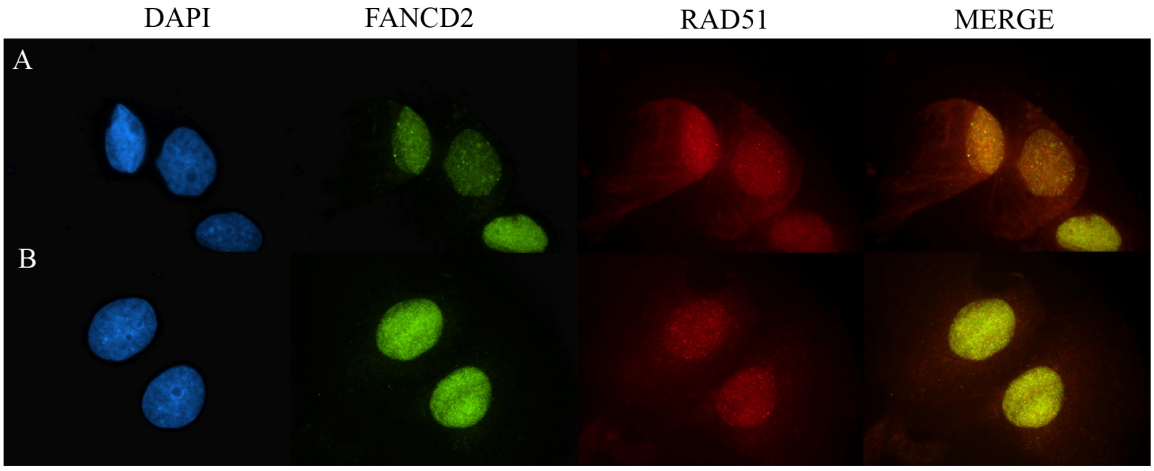

Figure 12. UPCI:SCC142 showing decreased FANCD2 and RAD51 focus formation.

Decreased FANCD2 and RAD51 focus formation in UPCI:SCC142 with and without exposure to 80ng/ml of MMC for 24 hr. **(A)** Untreated cells; **(B)** cells treated with 80 ng/mlof MMC showed decreased FANCD2 and RAD51 foci.

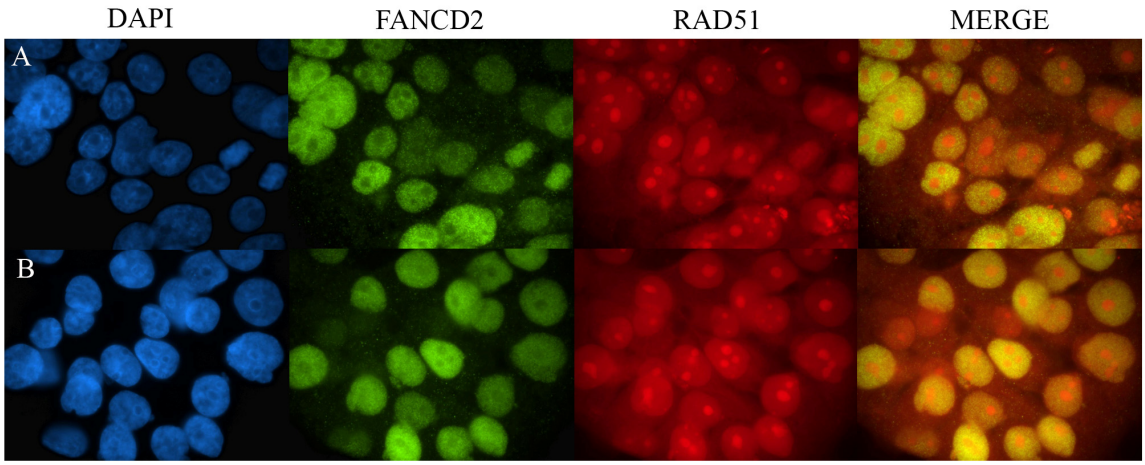

Figure 13. HNSCC derived from FA patient OHSU974 showing absence of FANCD2 and RAD51 focus formation.

Absence of FANCD2 and RAD51 focus formation in the HNSCC cell line derived from a FA patient. **(A)** Untreated cells; **(B)** cells treated with 80 ng/ml of MMC. The diffused brightness of the nuclei is caused by the inability of the cells to form FANCD2 foci.

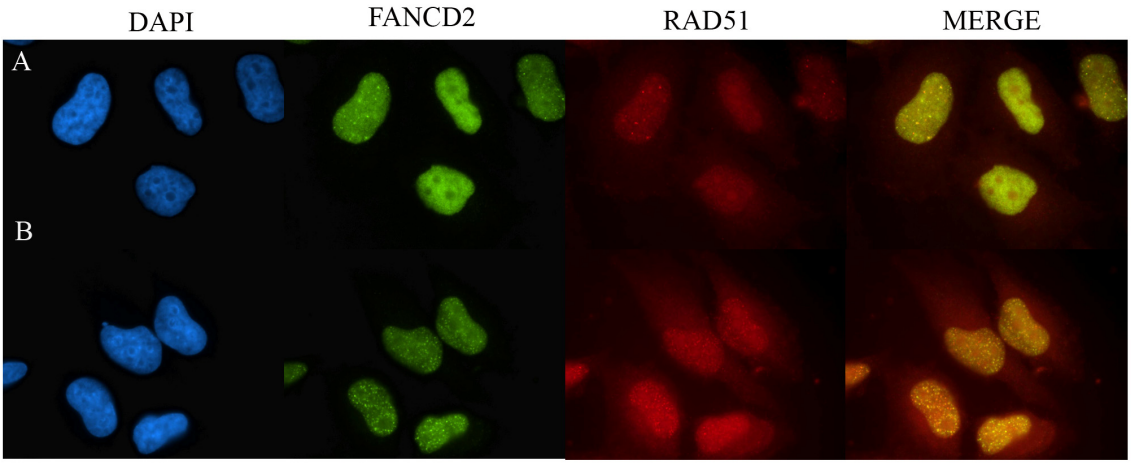

Figure 14. FA/BRCA pathway proficient cell line HeLa exhibiting FANCD2 and RAD51 focus formation.

FANCD2 and RAD51 focus formation in the FA/BRCA proficient HeLa cells with and without exposure to 80ng/ml of MMC for 24 hr. **(A)** Untreated cells; **(B)** cells treated with 80 ng/ml of MMC.

We observed that overall, the HNSCC cell lines exhibited a consistent pattern of *FANCD2* gene expression, FANCD2 monoubiquitination, and FANCD2 focus formation (Figure 15). The same pattern was observed in the HNSCC cell lines derived from FA patients and the FA/BRCA pathway proficient cell line. Only UPCI:SCC084, 104 and 131 showed increased FANCD2 monoubiquitination which does not coincides the observed decreased *FANCD2* gene expression and FANCD2 focus formation in each cell line.

Figure 15. Graph showing the L/S ratio of FANCD2 monoubiquitination, quantitation of *FANCD2* gene expression, and cells percentage of FANCD2 focus formation.

4.7 HNSCC CELL LINES DO NOT SURVIVE 10 GY IR

Our laboratory previously showed that HNSCC cell lines, particularly those with distal 11q loss, are radioresistant to 10 Gy and usually exhibit increased ATR and CHEK1 over expression along with decreased *TP53* expression (Parikh, et al unpublished data). HNSCC cell lines with distal 11q loss show also loss of the G_1 checkpoint as a result of a decreased TP53 expression, and an accumulation of the cell population at the G_2/M boundary upon exposure to IR. This enables HNSCC lines with 11q loss time to repair DNA damage before entering S phase or mitosis (Parikh, et al unpublished data). Previous data showed that inhibition of CHEK1 by siRNA radiosensitizes HNSCC cell lines with distal 11q loss. This is because inhibition of CHEK1 leads to the abrogation of the G2/M checkpoint and cell death of HNSCC with 11q loss (by premature chromatin condensation or mitotic catastrophe) by entering prematurely to S phase or M phase (Parikh et al, unpublished data). These previous observations make HNSCC with distal 11q loss a suitable candidate for CHEK1 Small Molecule Inhibitor (SMI) therapy. To determine the

radiosensitizing properties of a CHEK1 SMI, HNSCC cell lines were plated in 60 mm dishes for a clonogenic survival assay and exposed to different doses of SMI and IR. While performing the clonogenic survival assay, we did not observe cell survival at 10 Gy in HNSCC with 11q loss as observed previously in UPCI:SCC078, 131, and 136 (Parikh et al, unpublished data). We saw no cell survival in HNSCC cell lines without 11q13 amplification or 11q loss at 10 Gy. Despite these results, the percentage of survival in UPCI:SCC078 and 099 matched the previous results at 2.5 Gy (56% and 22%, respectively) and 5 Gy (10% and 3%, respectively) (Figures 16 and 17). This was not the case for UPCI:SCC131 and 136 which level of survival was decreased by 20 to 30% (Figures 18 and 19) from what was observed previously in our laboratory. Considering these findings, there are a couple of things to consider. First, it may be possible that the cell lines we have been working with are cross-contaminated with another cell line or the original vials were mislabeled. To illustrate this point, let's present an example. Imagine at some point in the past, there was a young college intern student in our laboratory helping a Ph.D. student with the tissue culture. He or she was assigned to prepare some HNSCC cells lines to cryopreserve in the liquid nitrogen tank for storage. At some point, someone walks into the room, asks him/her a question and he/she, unintentionally transfers the cells into the wrong cryovial. Later, he or she registers the vial in the liquid nitrogen tank log book. Back to the present, I pick that same vial thinking that I have the right cell line when in reality, it is not. Another possibility is that, cells could have undergone genetic changes after many passages that made them behave differently. Even though each cell line has been showing a unique pattern of growth and behavior in culture, which was easily recognized and suggests that they are the proper cell lines on which we have been working, a current effort is on its way to repeat these experiments in HNSCC cell lines at lower passage.

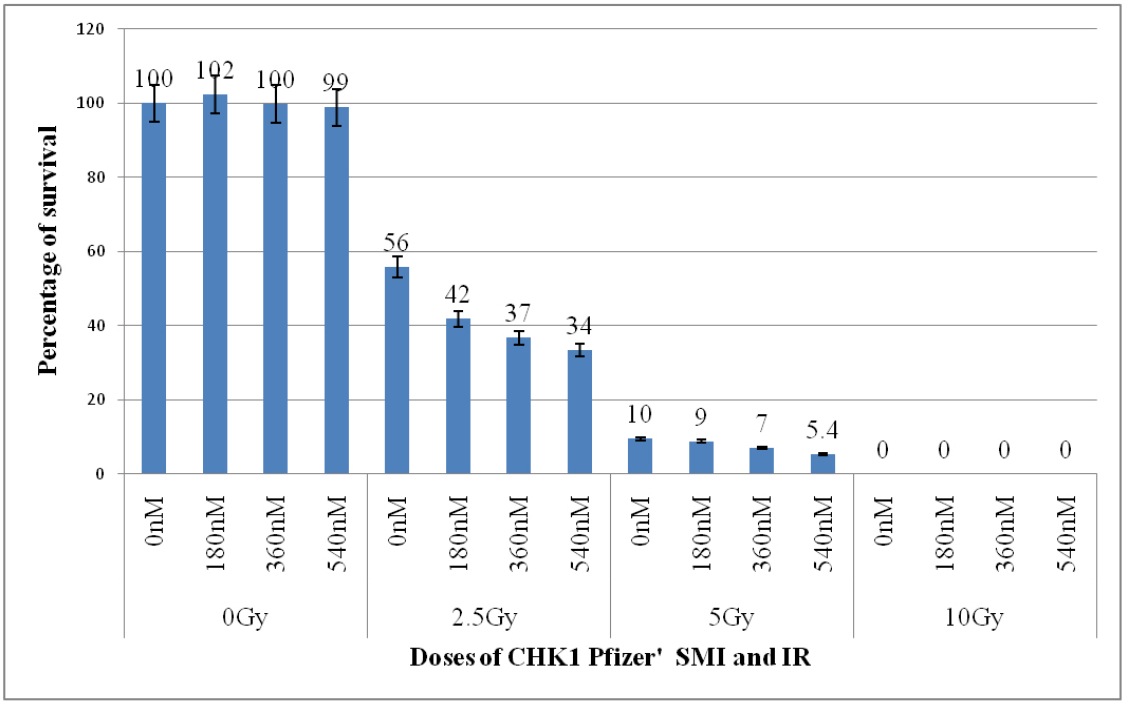

Figure 16. Clonogenic survival assay on UPCI:SCC078

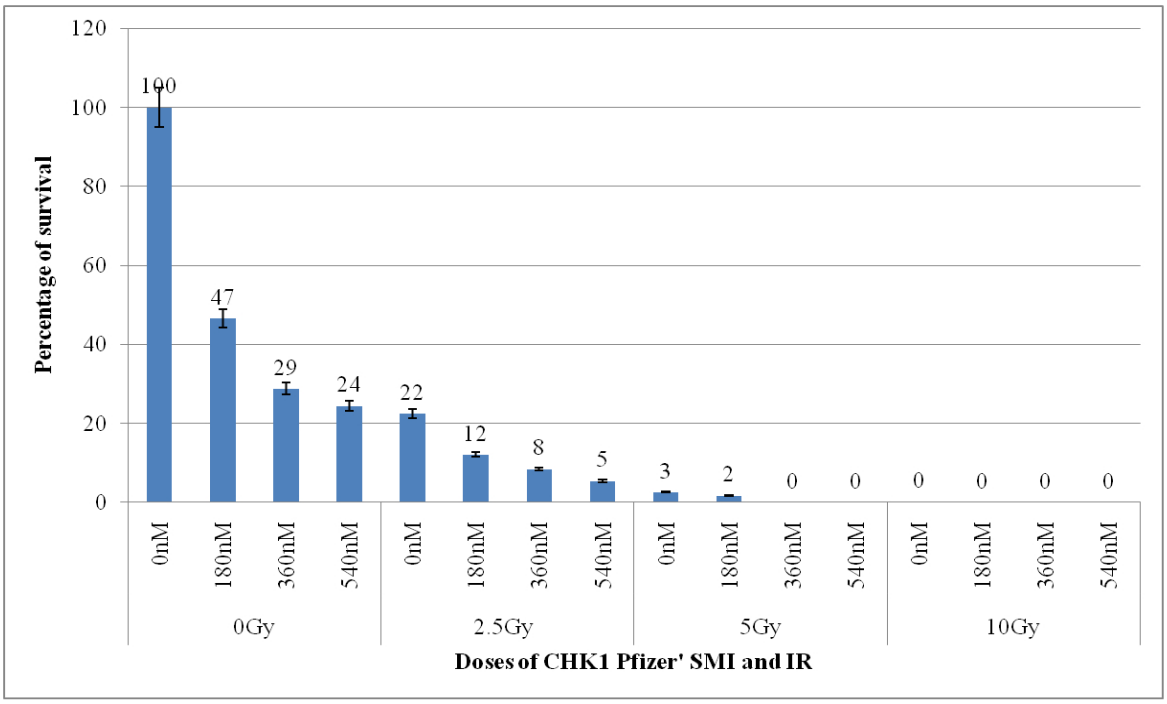

Figure 17. Clonogenic survival assay on UPCI:SCC099 after exposure to CHEK1 SMI and IR.

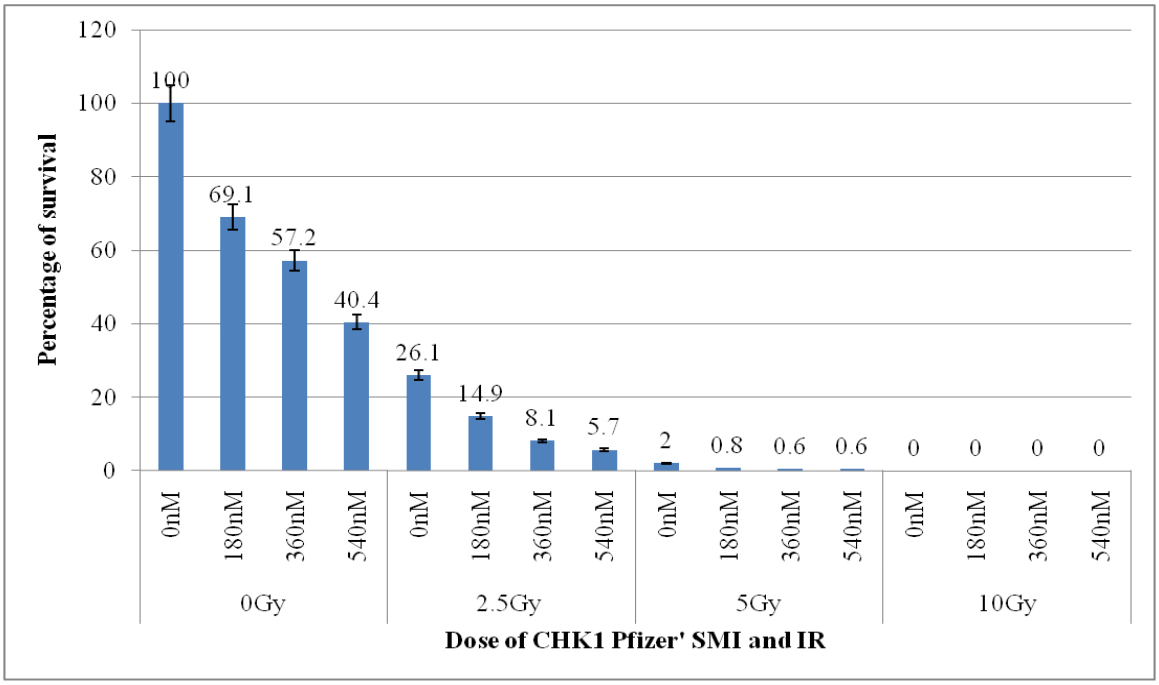

Figure 18. Clonogenic survival assay on UPCI:SCC131 after exposure to CHEK1 SMI and IR.

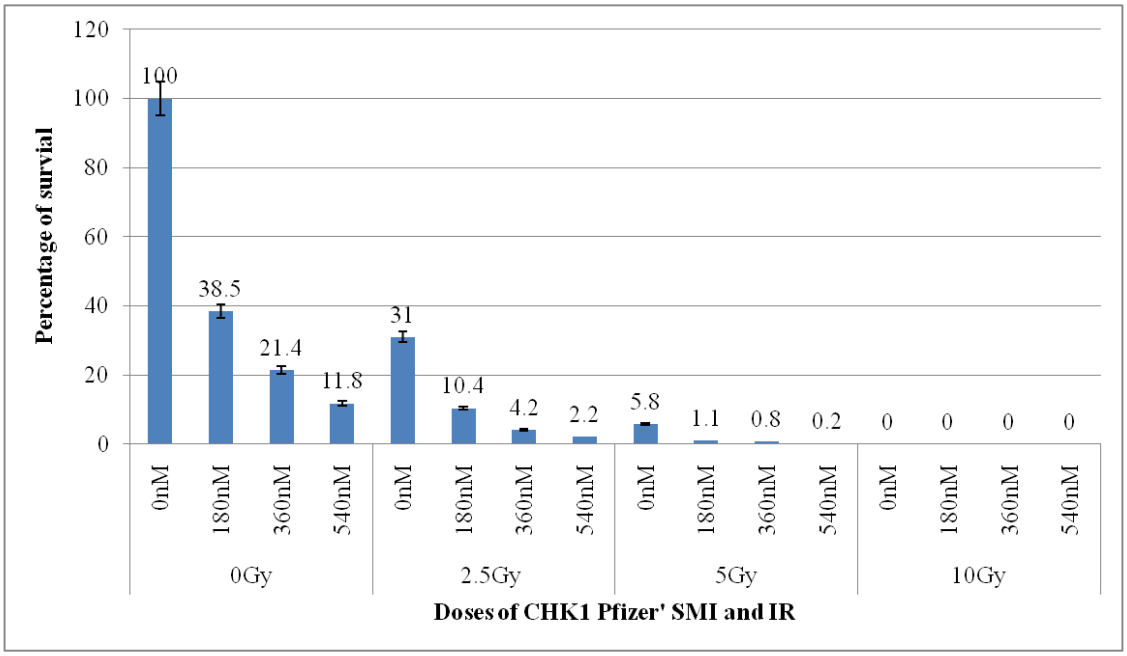

Figure 19. Clonogenic survival assay on UPCI:SCC136 after exposure to CHEK1 SMI and IR.

4.8 DECREASED CELL SURVIVAL IN TP53 MUTANT HNSCC CELL LINES AFTER EXPOSURE TO THE CHEK1 SMI

According to Blasina, the CHEK1 SMI is able to hypersensitize *TP53*-mutant cancer cells when administered along with a DNA damaging agent. This effect is not expected upon administration of the CHEK1 SMI alone for 24 hr (Blasina, et al. 2008). Blasina's group did not use a cell survival assay. Instead, when the cells reached 90% confluency (8 days after plating) they trypsinized the cells and counted them with a Coulter counter. To determine the radiosensitizing properties of the CHEK1 SMI, we plated HNSCC cell lines in 60 mm dishes for a clonogenic survival assay and exposed to different doses of SMI and IR. Despite their findings we observed

decreased cell survival in UPCI:SCC099, 131 and 136 (all of them TP53 deficient - Figure 20, A) upon exposure to the CHEK1 SMI alone. UPCI:SCC078, (TP53 proficient - Figure 20, A), did not show decreased cell survival upon exposure to the CHEK1 SMI alone.

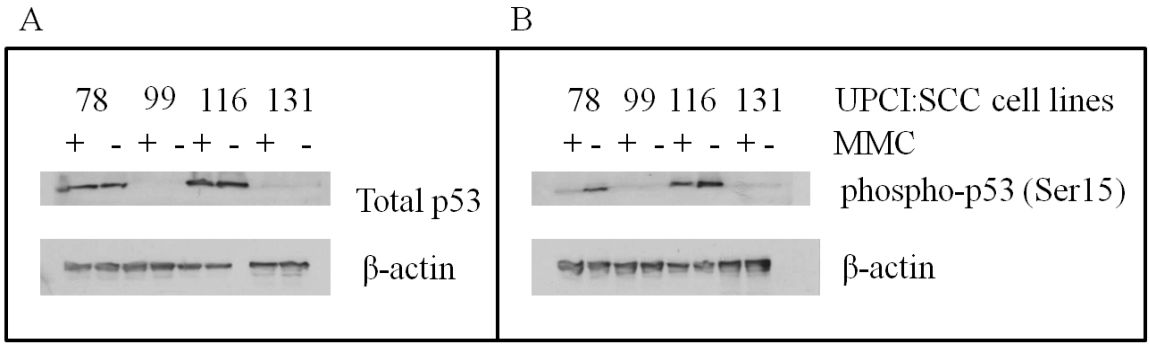

Figure 20. Western blotting for (A) total TP53 and (B) phospho-TP53 (ser15) in UPCI:SCC078, 099, 116 and 131 untreated and treated with 80 ng/ml MMC.

The administration of the CHEK1 SMI along with increasing doses of IR produced about 20 to 30% decreased cell survival in both TP53 deficient and proficient HNSCC cell lines. For the TP53 deficient HNSCC cell lines, this could indicate a potential radiosensitizing effect of the CHEK1 SMI. In the case of the TP53 proficient HNSCC cell line UPCI:SCC078, the CHEK1 SMI unexpectedly produced decreased cell survival when administered along with IR. This was unexpected because UPCI:SCC078 is a *TP53*-proficient cell line, bearing an intact G_1 checkpoint, which indicates that the CHEK1 SMI would not be able to abrogate the G_2/M checkpoint in this HNSCC cell line. We know by western blotting that UPCI:SCC078 is *TP53*-proficient (Figure 20, A). One way that the CHEK1 SMI could have radiosensitized UPCI:SCC078 is if the observed band in the TP53 western blot is a truncated version and therefore, nonfunctional. But, we can rule out this possibility based on the observation that TP53

can be phosphorylated in UPCI:SCC078 (Figure 20, B), confirming the functionality of TP53 and the ability of UPCI:SCC078 to bear an intact G_1 checkpoint.

4.9 THE CHEK1 SMI ABROGATES THE G2/M CHECKPOINT IN TP53-DEFICIENT HNSCC CELL LINES.

Blasina reported that upon exposure to the DNA damaging agent, Gemcitabine, TP53-deficient cancer cells showed a prominent S-phase arrest (Blasina, et al. 2008). This would have enabled the cancer cells to undergo DNA damage repair through the activation of the intra-S checkpoint or the G_2/M checkpoint before entering mitosis. Upon administration of the CHEK1 SMI, the S-phase arrest was decreased, yielding increased G_2/M and G_0-G_1 cell population (Blasina, et al. 2008). In UPCI:SCC078 (TP53 proficient), we did not see a noticeable change in the cell cycle profile, with and without either IR or the combination of CHEK1 SMI and IR, which would be expected in TP53-proficient cells. On the other hand, UPCI:SCC099 (TP53-deficient) showed about a 20% increase in the G_2/M cell population (Figure 21) at 5 Gy, indicating arrest at this point in the cell cycle, which was considerably reduced after exposure to the CHEK1 SMI. The observed increase in the G_2/M cell population is accompanied by an increase in the G1 cell population from 42% to 64%, indicating that the cancer cells are attempting to re-enter the cell cycle without undergoing DNA damage repair. It is also worth noting that when UPCI:SCC099 is exposed to the CHEK1 SMI, an increase in the G_2/M peak was also observed suggesting that in the absence of the G_1 checkpoint, the G_2/M checkpoint could be abrogated in TP53 deficient HNSCC cell lines like UPCI:SCC099 upon exposure to the CHEK1 SMI alone. Our results

indicate that the CHEK1 SMI overrides the G_2/M checkpoint in TP53 deficient HNSCC cell lines.

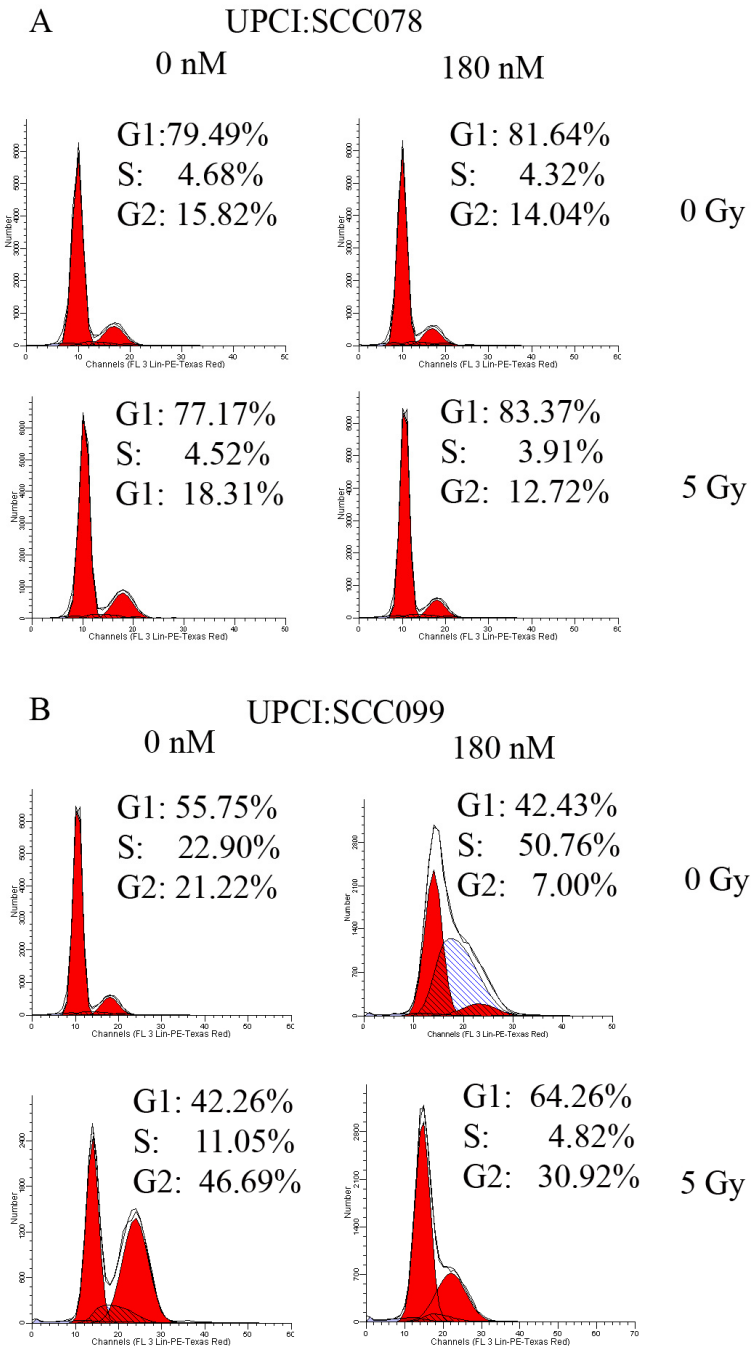

Figure 21. Cell cycle analysis of (A) UPCI:SCC078 (TP53 wild-type) and (B) 099 (TP53-mutant) treated and untreated with 5 Gy and 180 nM of CHEK1 SMI.

5.0 DISCUSSION

5.1 *FHIT* AND THE DEFECTIVE FA/BRCA PATHWAY IN HNSCC CELL LINES

One of the most frequent early alterations in HNSCC is 3p loss (Tsui, et al. 2008). The band, 3p14.2 is a hotspot for chromosome breakage and harbors a common fragile site, FRA3B, breakage of which can be induced by cigarette smoke, and other chemical compounds like aphidicolin (Durkin and Glover 2007; Stein, et al. 2002). FRA3B spans the tumor suppressor gene *FHIT*, and decreased FHIT protein expression is commonly observed in human cancers (Chang, et al. 2002; Huebner and Croce 2003) and is an indication of FRA3B breakage. FHIT is not the only tumor suppressor gene residing on the short arm of chromosome 3. FANCD2, part of the ID complex of the FA/BRCA pathway and required for the functionality of the pathway, is located distal to FRA3B at 3p25.3 (Hejna, et al. 2000). This means that upon breakage of FRA3B and a decreased FHIT protein expression, a segmental deletion of 3p could lead to *FANCD2* gene copy number loss. Despite the vast amount of evidence that shows that a decreased FHIT protein expression is common in human cancers (Huebner and Croce 2003), including breast (Yang, et al. 2001), lung (Sasaki, et al. 2006), cervix (Holschneider, et al. 2005), and HNSCC (Guerin, et al. 2006; Lee, et al. 2001; Virgilio, et al. 1996), it was just recently that D'Agostini showed that early loss of Fhit protein expression in the rat bronchial epithelium is induced by exposure to environmental cigarette smoke, suggesting that Fhit is a critical target of

environmental cigarette smoke (D'Agostini, et al. 2006). The observed decreased FHIT protein expression in around 85% of our HNSCC cell lines correlates with one of the first studies of the *FHIT* gene in HNSCC cell lines conducted shortly after its identification (Virgilio, et al. 1996). A review of the literature shows that the relationship between FRA3B breakage, 3p deletion, and FANCD2 loss has not been extensively investigated. A couple studies report that the short arm of chromosome 3 is one of the most frequently deleted genomic regions in esophageal cancer, which includes the tumor suppressor gene *FANCD2* as one of the top three genes deleted in that chromosome arm (Chen, et al. 2008; Sparano, et al. 2006). Moreover, only one study has evaluated the effect of an intact FA/BRCA pathway for a proper response to DNA replication stress (Howlett, et al. 2005). Howlett showed that disruption of the FA/BRCA pathway using FANCD2 siRNA in human colon cancer HCT116 cells resulted in 2–3-fold increased induction of chromosome gaps and breaks at both FRA3B and FRA16D fragile sites, as detected by FISH, at 0.2 and 0.4 μM APH, when compared with control siRNA transfected cells (Howlett, et al. 2005). To date, the relationship between FRA3B activation, 3p loss, *FANCD2* loss, and the DNA damage response through the FA/BRCA pathway has not been documented in human cancers, particularly HNSCC.

Our results demonstrate that decreased FHIT protein expression correlates with *FANCD2* gene copy loss and smoking history in HNSCC cell lines from patients with smoking history in ten of the fourteen HNSCC lines. Smoking and alcohol consumption history from the original patients from whom the HNSCC cell lines were derived is summarized in Table 4. The observation that *FANCD2* is lost in HNSCC cell lines correlates with previous studies in our laboratory in which 50% of the HNSCC cell lines studied showed 3p loss, highlighting the location of FANCD2 at this hot spot of genetic alterations (Martin, et al. 2008). Even though we

do not know the smoking history of the FA patients from whom HNSCC cell lines OHSU974 and VU1365 were derived, the observed decreased FHIT protein in these cell lines correlates with the observed decreased FHIT protein expression in the sporadic HNSCC cell lines. This suggests that breakage 3p14.2, the location of FRA3B/*FHIT*, is also plausible in these cell lines, possibly due to their DNA damage response defects. Howlett showed that disruption of the FA/BRCA pathway using FANCD2 siRNA in human colon cancer HCT116 cells resulted in 2–3-fold increased induction of chromosome gaps and breaks at both FRA3B and FRA16D fragile sites (Howlett, et al. 2005). These results suggest that an intact FA/BRCA pathway is required to prevent FRA3B breakage. Therefore, *FANCD2* loss could lead to a decreased ability of the cells to prevent FRA3B breakage upon exposure to environmental insults like cigarette smoke. On the other hand, HPV integration could be a source of FRA3B breakage. On the other hand, DNA sites of viral integration could promote FRA3B breakage. The Human papillomavirus has been associated with FRA3B breakage (Ohta, et al. 1996). But, considering that only UPCI:SCC099 is HPV positive leaves this possibility on the side as a possible mechanism leading to breakage at 3p14.2 and decreased FHIT protein expression in the FA patient derived and our HNSCC cell lines.

Only two sporadic HNSCC cell lines, UPCI:SCC078 and 104 showed FHIT protein expression, which suggests that there is no breakage at 3p14.2. Despite this observation UPCI:SCC078 and 104 still exhibited *FANCD2* gene copy number loss. First, this discordant observation could be due to an actual breakage in the *FHIT* gene leading to a mutant truncated form of the FHIT protein, detectable by western blot (Kisielewski, et al. 1998) and further loss of *FANCD2*. This scenario is plausible, based on previous studies in our laboratory that have shown by FISH that *FHIT* exon 10 is lost in 90% of the cells in both UPCI:SCC78 and 104 (White, et

al. unpublished data). The formation of aberrant *FHIT* transcripts able to encode partial proteins with or without the HIT domain is also possible through an in-frame methionine codon in exon 6 (Ohta, et al. 1996; Virgilio, et al. 1996). Another possibility could be that despite 3p deletion, then *FHIT* gene may not be deleted. This assumption is based on Maestros' investigations in which they mapped three commonly deleted regions at 3p (3p24-ter, 3p21.3, and 3p14-cen). Therefore, if 3p loss occurs at either 3p24-pter or 3p21.3, *FANCD2* could be deleted while *FHIT* remains intact (Maestro, et al. 1993). On other hand, only two sporadic HNSCC cell lines, UPCI:SCC066 and 103 show decreased FHIT expression without FANCD2 gene copy number loss, which could be due to the inactivation of the *FHIT* gene by promoter methylation (Chang, et al. 2002). This eventually could lead to a decreased FHIT protein expression, suggesting that, in the absence of FRA3B breakage *FANCD2* would not be deleted as detected by FISH.

Fifty percent of the HNSCC cell lines derived from patients with smoking history showed decreased FHIT expression and *FANCD2* gene copy loss which also correlates with decreased induction of *FANCD2* gene expression. Even though FHIT-deficient HNSCC cell lines did not exhibit a noticeable decrease in *FANCD2* baseline expression (Figure 6), we observed overall decreased induction of the *FANCD2* gene expression upon exposure to MMC as shown in Figure 7. The lack of a noticeable decrease in *FANCD2* baseline expression seems plausible when considering the ploidy of the HNSCC cell lines (Table 4). The majority of the HNSCC cell lines show a ploidy ranging from 2 to 5. Therefore, HNSCC cell lines, like UPCI:SCC104, which has a ploidy of 4 to 5 may have lost two copies of FANCD2, leaving it with three copies of the gene. Regarding the decreased induction of *FANCD2* gene expression, it could be due to constitutive activation of *FANCD2* in HNSCC cell lines in response to the constantly generated endogenous chromosomal instability possibly originated by numerous structural and numerical aberrations.

After all, chromosomal instability is one of the most characteristic features of HNSCC cell lines (Reshmi and Gollin 2005). After exposure to an additional external source of DNA damage, like MMC, HNSCC cell lines already experiencing chromosomal instability will have minimal induction of *FANCD2* gene expression due to the constitutively high *FANCD2* gene expression.

Overall decreased FANCD2 protein expression, ranging from mildly to moderately decreased was also characteristic of FHIT-deficient HNSCC cell lines. Three HNSCC cell lines (UCPI:SCC084, 104 and 142) which showed mildly decreased FANCD2 protein expression correlated well with the observed decreased FHIT protein expression, decreased baseline and induced *FANCD2* gene expression and gene copy loss. This was not the case for UPCI:SCC066 and 078, which showed moderately decreased FANCD2 protein expression. Even though UPCI:SCC066 showed decreased FHIT expression and mildly decreased FANCD2 protein expression, it does not show *FANCD2* gene copy loss or decreased FANCD2 baseline gene expression. Although, it has not been reported yet, *FANCD2* promoter methylation could explain the observed moderately decreased FANCD2 protein expression in UPCI:SCC066. But, then *FANCD2* gene expression should be lower in this cell line, which is not the case. UPCI:SCC066 show almost 2-fold increased FANCD3 basal expression compared to the FA/BRCA proficient HeLa cell line (Figure 6). On the other hand, despite the observation of *FANCD2* gene copy loss and mildly decreased FANCD2 protein expression, UPCI:SCC078 showed FHIT expression which indicates no 3p14.2 breakage. Considering that UPCI:SCC078 was derived from a patient without a smoking history, exposure of the patient to environmental cigarette smoke could have triggered 3p loss at either 3p24-pter or 3p21.3, leading to deletion of *FANCD2* and intact *FHIT* gene (Maestro, et al. 1993).

The ability of the FHIT protein-deficient HNSCC cells to form FANCD2 foci after exposure to MMC was not compromised, except in UPCI:SCC105 and 116. Decreased FANCD2 monoubiquitination can be observed in cell lines derived from FA patients lacking one of the protein members of the core complex. The integrity of the FA core complex is required for FANCD2 monoubiquitination as it is supposed to be the ubiquitin ligase (E3) for FANCD2 monoubiquitination (Taniguchi, et al. 2002). Moreover, although the mechanisms responsible for the inhibition of FANCD2 monoubiquitination remain unclear, the importance of the deubiquitinating has been suggested of the enzyme, USP1, which deubiquitinates monoubiquitinated FANCD2 and negatively regulates the Fanconi anemia pathway (Jacquemont and Taniguchi 2007). Our results resolve the above mentioned possibilities to explain the observed decreased FANCD2 monoubiquitination in HNSCC cell lines.

Recruitment of FANCD2 to the DNA damage site, by focus formation, is an indication of an intact FA core complex and functional FA/BRCA pathway required for the assembly of the repair complex (BRCA1, BRCA2, RAD51) for DNA damage repair (Hussain, et al. 2004; Taniguchi, et al. 2002). FHIT deficient HNSCC cell lines showed decreased FANCD2 and RAD51 focus formation. It is worth noting that not all the cells within a cell line showed a uniform response to MMC compared to the FA/BRCA proficient HeLa cell line. In Figure 11, we can see that while some cells in the microscopic field showed both FANCD2 and RAD51 focus formation, others do not. This observation could indicate that a subset of HNSCC cells within a cell population may be actually FHIT deficient with the corresponding *FANCD2* gene copy loss, decreased *FANCD2* gene and protein expression, and ultimately, a decreased ability to form FANCD2 and RAD51 foci. Furthermore, this could also imply that upon exposure to MMC, only a subset of HNSCC cells within a cell population could be able to repair DNA

damage via activation of the FA/BRCA pathway. The remaining cell population may be unable to activate DNA damage repair and would eventually accumulate so many genetic alterations that it would eventually undergo apoptosis.

When considering all of the data together, *FANCD2* gene expression, protein monoubiquitination and focus formation, we observed that UPCI:SCC084 and 104 exhibited increased FANCD2 monoubiquitination compared to the other HNSCC cell lines studied, including the FA/BRCA proficient cell line. Could it be possible that UPCI:SCC084 and 104 are experiencing higher induction of FANCD2 monoubiquitination? 11q13 amplification is a common event in HNSCC, leading to the overexpression of genes clustered in that chromosomal region, including cyclin D1 (*CCND1*), tumor amplified and overexpressed sequence 1 (*TAOS1*) and protein phosphatase 1alpha (*PPP1CA*) (Hsu, et al. 2006). Interestingly, the RAD9 protein is part of the 9-1-1 complex and an early activator of ATR also located at 11q13.1-13.2 (Lieberman, et al. 1996). RAD9 has been reported to be necessary for proper activation of the FA/BRCA pathway upon exposure to DNA damage, particularly by regulating FANCD2 monoubiquitination as shown by siRNA experiments (Guervilly, et al. 2008). By interrogating a small subset of HNSCC cell lines for RAD9 protein expression, we found out that UPCI:SCC084 and 104 showed 1.5 and 1.4-fold increased RAD9 protein expression respectively by western blot (Figure 22). Then, based on this observation the possibility exists that RAD9 increased protein expression may be promoting the increased induction of FANCD2 monoubiquitination in UPCI:SCC078 and 104 upon exposure to MMC. It is worth noting that UPCI:SCC029B and 66 showed 1.7 and 1.2-fold increased RAD9 protein expression, which does not seem influence the FANCD2 monoubiquitination.

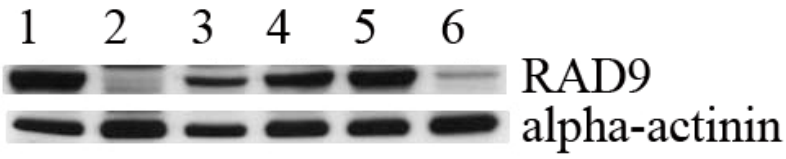

Figure 22. RAD9 protein expression in HNSCC cell lines and the HEK293 cell line.

Immunoblotting was performed to detect protein expression levels for RAD9. We observed increased protein expression in HNSCC cell lines **(1)** UPCI:SCC029B, **(3)** 066, **(4)** 084, and **(5)** 104. Decreased protein expression was observed in **(2)** 040. **(6)** HEK293 was used as a control.

5.2 CHEK1 INHIBITION AND A DEFECTIVE FA/BRCA PATHWAY IN HNSCC CELL LINES

There is increasing interest for using CHEK1 inhibitors as chemotherapeutic agents in cancer treatment (Zhang, et al. 2009). The FA/BRCA pathway is activated through a downstream phosphorylation cascade mediated by either the ATM or ATR kinase and downstream effectors like CHEK1 to phosphorylate key FA core complex proteins like FANCM (Collis, et al. 2008) and FANCE (Wang, et al. 2007). Upon inhibition of CHEK1 by siRNA, FANCD2 monoubiquitination was impaired in HNSCC as recently described (Chen, et al. 2009), where FANCD2 deficient cells were hypersensitive to CHEK1 inhibition. It could be possible that the observed radiosensitizing properties of CHEK1 inhibition in HNSCC cell lines could be due in part to the further deregulation of an already defective FA/BRCA pathway.

The administration of CHEK1 SMI in HNSCC cell lines induces radiosensitization and changes in the cell cycle. Previously in our laboratory, it has been observed that upon treatment

with IR, HNSCC cell lines with distal 11q loss showed accumulation of cells in G_2/M. Inhibition of CHEK1 by siRNA in HNSCC cell lines with distal 11q loss caused a reduction in the accumulation of cells in G_2/M and increased radiosensitivity. On the other hand, HNSCC cell lines without distal 11q loss treated with IR showed a modest G_2/M accumulation compared to HNSCC cell lines with distal 11q loss and modest radiosensitivity. Inhibition of CHEK1 by siRNA in HNSCC cell lines without distal 11q loss did not cause G_2/M accumulation (Parikh et al, unpublished data). Interestingly, after treating HNSCC cell lines with IR and the CHEK1 SMI we observed the opposite effect. When treated with IR only, HNSCC cell lines without distal 11q loss, i.e., UPCI:SCC099 showed increased accumulation of cells at G_2/M (from 21% to 46%) as compared to the HNSCC cell lines with distal 11q loss (from 15% to 18%). After the administration of the CHEK1 SMI and IR, HNSCC cell lines without distal 11q loss showed a decreased accumulation of cells in G_2/M (from 46% to 30) as compared to the HNSCC cell lines with distal 11q loss (from 18% to 14%). The administration of the CHEK1 SMI along with increasing doses of IR produced 20 to 30% decreased cell survival in all HNSCC cell lines.

It is important to note these results while taking into consideration a couple of characteristics exhibited by these cell lines, the TP53 status and FHIT protein expression. Western blotting studies showed that UPCI:SCC078 has wild type TP53, while UPCI:SCC099 exhibited decreased TP53 protein expression. Also, UPCI:SCC078 showed FHIT protein expression compared to decreased FHIT expression shown by UPCI:SCC099. Hu showed in epithelial cells from mouse kidney that Fhit $^{-/-}$ cells have an over-activated ATR-CHK1 pathway which allows them to accumulate in G_2 after exposure to IR. The strong S and G2 response facilitated homologous recombination repair and radioresistance to Fhit $^{-/-}$ cells. After treatment with either ATR or CHEK1 siRNA, Fhit $^{-/-}$ cells were radiosensitized, concluding that the

radioresistant phenotype observed in Fhit $^{-/-}$ cells depends on a strong checkpoint response (Hu, et al. 2005). Parikh performed QPCR and western blotting for ATR and CHEK1 in UPCI:SCC099 showing that the ATR-CHK1 pathway was not over-activated (Parikh et al, unpublished data). It appears that decreased FHIT protein expression does not correlate well with an over-activated ATR-CHK1 pathway in HNSCC cell lines. Considering the TP53 protein expression in HNSCC cell lines, we see a correlation between the observed changes in the cell cycle and radiosensitization in UPCI:SCC099 (TP53 mutant) compared to UPCI:SCC078 (TP53 wild-type) upon exposure to the CHEK1 SMI. These observations agreed with the expected specific effect of the CHEK1 SMI on TP53 mutant cancer cells (Blasina, et al. 2008).

Finally, it could be possible that the high levels of chromosomal instability (an endogenous DNA damaging event) experienced by HNSCC cell lines (Reshmi and Gollin 2005) together with the administration of CHEK1 SMI may explain why we see decreased cell survival when the UPCI:SCC099 and 131 cell lines are exposed to the CHEK1 SMI alone. Our results demonstrate that a defective FA/BRCA pathway prevails in HNSCC cell lines derived from patients who smoked. These cell lines are mainly characterized by *FANCD2* gene copy loss which correlates with decreased FHIT protein expression suggesting 3p14.2 loss. Thus, we propose that smoking may play a role in the observed decreased FHIT expression, 3p14.2 deletion, *FANCD2* gene copy loss and consequently, the defective FA/BRCA pathway.

Several questions pertaining to this study remain unanswered which could have contributed to its completeness. First, does the decreased FANCD2 and RAD51 focus formation observed in HNSCC cell lines make these cells more sensitive to inter-strand crosslinking agents like MMC? This question could have been answered by performing a MMC sensitivity assay as previously described (Taniguchi, et al. 2002) with an expected increased sensitivity in those

HNSCC cell lines with decreased FANCD2 and RAD51 focus formation. Second, considering the heterogeneous cell population in each HNSCC cell line, are those cells exhibiting absent FANCD2 and RAD51 focus formation proficient for the components of the DNA repair complex of the FA/BRCA pathway, named BRCA1, BRCA2/FANCD1, FANCJ or FANCN? By using Laser Capture Microdissection (LCM) we could have been able to separate HNSCC cell lines that showed no FANCD2/RAD51 formation from those exhibiting foci formation and study them in parallel. This could provide a better understanding the heterogeneity of the cell population in each cell line, potentially useful information when considering therapeutic strategies in such complex cell populations. Therefore, further investigation of the FA/BRCA pathway in HNSCC is warranted.

6.0 PUBLIC HEALTH SIGNIFICANCE

Head and neck squamous cell carcinoma (HNSCC) is a clear example of a type of cancer whose origin is caused by environmental factors like smoking and alcohol. Smoking itself is a serious public health issue that has been associated with chromosomal instability in HNSCC. Investigating the molecular mechanisms behind the influence of environmental factors in the genesis of cancer could improve our understanding of this enigmatic disease. The loss of the short arm of chromosome 3 (3p) is one of the most frequent events in HNSCC and it has been linked to smoking and the activation of the common fragile site, FRA3B. Our results demonstrate that FRA3B was likely activated in HNSCC cell lines which show decreased FHIT protein expression. This observation correlates with *FANCD2* gene copy loss and abnormal DNA damage repair. The use of targeted therapy on cancer cells with deficient DNA damage repair could improve the currently available cancer treatment schemes. As an example, targeted inhibition of *CHEK1*, an important mediator of the G2/M cell cycle checkpoint, not only disrupts the previously mentioned checkpoint but also could disrupts the FA/BRCA pathway in cancer cells by inhibiting the phosphorylation of CHEK1 downstream targets like FANCE, FANCM and FANCD2, leading to chemo- or radiosensitization. Therefore, an abnormal FA/BRCA pathway could be used as a marker for selective use of targeted cancer therapy for HNSCC.

BIBLIOGRAPHY

Bartek J, Lukas J. 2007. DNA damage checkpoints: from initiation to recovery or adaptation. Curr Opin Cell Biol 19(2):238-45.

Blasina A, Hallin J, Chen E, Arango ME, Kraynov E, Register J, Grant S, Ninkovic S, Chen P, Nichols T and others. 2008. Breaching the DNA damage checkpoint via PF-00477736, a novel small-molecule inhibitor of checkpoint kinase 1. Mol Cancer Ther 7(8):2394-404.

Carvalho AL, Nishimoto IN, Califano JA, Kowalski LP. 2005. Trends in incidence and prognosis for head and neck cancer in the United States: a site-specific analysis of the SEER database. Int J Cancer 114(5):806-16.

Castellsague X, Quintana MJ, Martinez MC, Nieto A, Sanchez MJ, Juan A, Monner A, Carrera M, Agudo A, Quer M and others. 2004. The role of type of tobacco and type of alcoholic beverage in oral carcinogenesis. Int J Cancer 108(5):741-9.

Chang KW, Kao SY, Tzeng RJ, Liu CJ, Cheng AJ, Yang SC, Wong YK, Lin SC. 2002. Multiple molecular alterations of FHIT in betel-associated oral carcinoma. J Pathol 196(3):300-6.

Chen CC, Kennedy RD, Sidi S, Look AT, D'Andrea A. 2009. CHK1 inhibition as a strategy for targeting Fanconi Anemia (FA) DNA repair pathway deficient tumors. Mol Cancer 8:24.

Chen J, Guo L, Peiffer DA, Zhou L, Chan OT, Bibikova M, Wickham-Garcia E, Lu SH, Zhan Q, Wang-Rodriguez J and others. 2008. Genomic profiling of 766 cancer-related genes in archived esophageal normal and carcinoma tissues. Int J Cancer 122(10):2249-54.

Collis SJ, Ciccia A, Deans AJ, Horejsi Z, Martin JS, Maslen SL, Skehel JM, Elledge SJ, West SC, Boulton SJ. 2008. FANCM and FAAP24 function in ATR-mediated checkpoint signaling independently of the Fanconi anemia core complex. Mol Cell 32(3):313-24.

D'Agostini F, Izzotti A, Balansky R, Zanesi N, Croce CM, De Flora S. 2006. Early loss of Fhit in the respiratory tract of rodents exposed to environmental cigarette smoke. Cancer Res 66(7):3936-41.

Darzynkiewicz Z, Juan G. 2001. DNA content measurement for DNA ploidy and cell cycle analysis. Curr Protoc Cytom Chapter 7:Unit 7 5.

Druck T, Hadaczek P, Fu TB, Ohta M, Siprashvili Z, Baffa R, Negrini M, Kastury K, Veronese ML, Rosen D and others. 1997. Structure and expression of the human FHIT gene in normal and tumor cells. Cancer Res 57(3):504-12.

Durkin SG, Arlt MF, Howlett NG, Glover TW. 2006. Depletion of CHK1, but not CHK2, induces chromosomal instability and breaks at common fragile sites. Oncogene 25(32):4381-8.

Durkin SG, Glover TW. 2007. Chromosome fragile sites. Annu Rev Genet 41:169-92.

Franken NA, Rodermond HM, Stap J, Haveman J, van Bree C. 2006. Clonogenic assay of cells in vitro. Nat Protoc 1(5):2315-9.

Garcia-Higuera I, Taniguchi T, Ganesan S, Meyn MS, Timmers C, Hejna J, Grompe M, D'Andrea AD. 2001. Interaction of the Fanconi anemia proteins and BRCA1 in a common pathway. Mol Cell 7(2):249-62.

Green AM, Kupfer GM. 2009. Fanconi anemia. Hematol Oncol Clin North Am 23(2):193-214.

Guerin LA, Hoffman HT, Zimmerman MB, Robinson RA. 2006. Decreased fragile histidine triad gene protein expression is associated with worse prognosis in oral squamous carcinoma. Arch Pathol Lab Med 130(2):158-64.

Guervilly JH, Mace-Aime G, Rosselli F. 2008. Loss of CHK1 function impedes DNA damage-induced FANCD2 monoubiquitination but normalizes the abnormal G2 arrest in Fanconi anemia. Hum Mol Genet 17(5):679-89.

Haddad RI, Shin DM. 2008. Recent advances in head and neck cancer. N Engl J Med 359(11):1143-54.

Hays LE, Zodrow DM, Yates JE, Deffebach ME, Jacoby DB, Olson SB, Pankow JF, Bagby GC. 2008. Cigarette smoke induces genetic instability in airway epithelial cells by suppressing FANCD2 expression. Br J Cancer 98(10):1653-61.

Hejna JA, Timmers CD, Reifsteck C, Bruun DA, Lucas LW, Jakobs PM, Toth-Fejel S, Unsworth N, Clemens SL, Garcia DK and others. 2000. Localization of the Fanconi anemia complementation group D gene to a 200-kb region on chromosome 3p25.3. Am J Hum Genet 66(5):1540-51.

Holschneider CH, Baldwin RL, Tumber K, Aoyama C, Karlan BY. 2005. The fragile histidine triad gene: a molecular link between cigarette smoking and cervical cancer. Clin Cancer Res 11(16):5756-63.

Howlett NG, Taniguchi T, Durkin SG, D'Andrea AD, Glover TW. 2005. The Fanconi anemia pathway is required for the DNA replication stress response and for the regulation of common fragile site stability. Hum Mol Genet 14(5):693-701.

Hsu LC, Huang X, Seasholtz S, Potter DM, Gollin SM. 2006. Gene amplification and overexpression of protein phosphatase 1alpha in oral squamous cell carcinoma cell lines. Oncogene 25(40):5517-26.

Hu B, Han SY, Wang X, Ottey M, Potoczek MB, Dicker A, Huebner K, Wang Y. 2005. Involvement of the Fhit gene in the ionizing radiation-activated ATR/CHK1 pathway. J Cell Physiol 202(2):518-23.

Huang X, Gollin SM, Raja S, Godfrey TE. 2002. High-resolution mapping of the 11q13 amplicon and identification of a gene, TAOS1, that is amplified and overexpressed in oral cancer cells. Proc Natl Acad Sci U S A 99(17):11369-74.

Huebner K, Croce CM. 2003. Cancer and the FRA3B/FHIT fragile locus: it's a HIT. Br J Cancer 88(10):1501-6.

Huebner K, Hadaczek P, Siprashvili Z, Druck T, Croce CM. 1997. The FHIT gene, a multiple tumor suppressor gene encompassing the carcinogen sensitive chromosome fragile site, FRA3B. Biochim Biophys Acta 1332(3):M65-70.

Hussain S, Wilson JB, Medhurst AL, Hejna J, Witt E, Ananth S, Davies A, Masson JY, Moses R, West SC and others. 2004. Direct interaction of FANCD2 with BRCA2 in DNA damage response pathways. Hum Mol Genet 13(12):1241-8.

Ishii H, Mimori K, Inoue H, Inageta T, Ishikawa K, Semba S, Druck T, Trapasso F, Tani K, Vecchione A and others. 2006. Fhit modulates the DNA damage checkpoint response. Cancer Res 66(23):11287-92.

Jacquemont C, Taniguchi T. 2007. Proteasome function is required for DNA damage response and fanconi anemia pathway activation. Cancer Res 67(15):7395-405.

Jemal A, Siegel R, Ward E, Hao Y, Xu J, Murray T, Thun MJ. 2008. Cancer statistics, 2008. CA Cancer J Clin 58(2):71-96.

Kalb R, Neveling K, Herterich S, Schindler D. 2007. Fanconi anemia genes: structure, mutations, and genotype-phenotype correlation. In: Hoehn H, Schindler D, editor. Fanconi Anemia. A Paradigmatic Disease for the Understanding of Cancer and Aging. Basel: Karger. p 39-58.

Kisielewski AE, Xiao GH, Liu SC, Klein-Szanto AJ, Novara M, Sina J, Bleicher K, Yeung RS, Goodrow TL. 1998. Analysis of the FHIT gene and its product in squamous cell carcinomas of the head and neck. Oncogene 17(1):83-91.

Le Beau MM, Drabkin H, Glover TW, Gemmill R, Rassool FV, McKeithan TW, Smith DI. 1998. An FHIT tumor suppressor gene? Genes Chromosomes Cancer 21(4):281-9.

Lee JI, Soria JC, Hassan K, Liu D, Tang X, El-Naggar A, Hong WK, Mao L. 2001. Loss of Fhit expression is a predictor of poor outcome in tongue cancer. Cancer Res 61(3):837-41.

Lieberman HB, Hopkins KM, Nass M, Demetrick D, Davey S. 1996. A human homolog of the Schizosaccharomyces pombe rad9+ checkpoint control gene. Proc Natl Acad Sci U S A 93(24):13890-5.

Maestro R, Gasparotto D, Vukosavljevic T, Barzan L, Sulfaro S, Boiocchi M. 1993. Three discrete regions of deletion at 3p in head and neck cancers. Cancer Res 53(23):5775-9.

Maitra A, Wistuba, II, Washington C, Virmani AK, Ashfaq R, Milchgrub S, Gazdar AF, Minna JD. 2001. High-resolution chromosome 3p allelotyping of breast carcinomas and precursor lesions demonstrates frequent loss of heterozygosity and a discontinuous pattern of allele loss. Am J Pathol 159(1):119-30.

Martin CL, Reshmi SC, Ried T, Gottberg W, Wilson JW, Reddy JK, Khanna P, Johnson JT, Myers EN, Gollin SM. 2008. Chromosomal imbalances in oral squamous cell carcinoma: examination of 31 cell lines and review of the literature. Oral Oncol 44(4):369-82.

Matsumoto S, Kasumi F, Sakamoto G, Onda M, Nakamura Y, Emi M. 1997. Detailed deletion mapping of chromosome arm 3p in breast cancers: a 2-cM region on 3p14.3-21.1 and a 5-cM region on 3p24.3-25.1 commonly deleted in tumors. Genes Chromosomes Cancer 20(3):268-74.

Motoyama N, Naka K. 2004. DNA damage tumor suppressor genes and genomic instability. Curr Opin Genet Dev 14(1):11-6.

Negri E, La Vecchia C, Franceschi S, Tavani A. 1993. Attributable risk for oral cancer in northern Italy. Cancer Epidemiol Biomarkers Prev 2(3):189-93.

Ohta M, Inoue H, Cotticelli MG, Kastury K, Baffa R, Palazzo J, Siprashvili Z, Mori M, McCue P, Druck T and others. 1996. The FHIT gene, spanning the chromosome 3p14.2 fragile site and renal carcinoma-associated t(3;8) breakpoint, is abnormal in digestive tract cancers. Cell 84(4):587-97.

Olshan AF, Weissler MC, Watson MA, Bell DA. 2000. GSTM1, GSTT1, GSTP1, CYP1A1, and NAT1 polymorphisms, tobacco use, and the risk of head and neck cancer. Cancer Epidemiol Biomarkers Prev 9(2):185-91.

Parikh RA, White JS, Huang X, Schoppy DW, Baysal BE, Baskaran R, Bakkenist CJ, Saunders WS, Hsu LC, Romkes M and others. 2007. Loss of distal 11q is associated with DNA repair deficiency and reduced sensitivity to ionizing radiation in head and neck squamous cell carcinoma. Genes Chromosomes Cancer 46(8):761-75.

Parkin DM, Bray F, Ferlay J, Pisani P. 2005. Global cancer statistics, 2002. CA Cancer J Clin 55(2):74-108.

Poschl G, Seitz HK. 2004. Alcohol and cancer. Alcohol Alcohol 39(3):155-65.

Reshmi SC, Gollin SM. 2005. Chromosomal instability in oral cancer cells. J Dent Res 84(2):107-17.

Rosenberg PS, Alter BP, Ebell W. 2008. Cancer risks in Fanconi anemia: findings from the German Fanconi Anemia Registry. Haematologica 93(4):511-7.

Rosenberg PS, Greene MH, Alter BP. 2003. Cancer incidence in persons with Fanconi anemia. Blood 101(3):822-6.

Sasaki H, Haneda H, Yukiue H, Kobayashi Y, Yano M, Fujii Y. 2006. Decreased fragile histidine triad gene messenger RNA expression in lung cancer. Clin Lung Cancer 7(6):412-6.

Shaw G, Morse S, Ararat M, Graham FL. 2002. Preferential transformation of human neuronal cells by human adenoviruses and the origin of HEK 293 cells. FASEB J 16(8):869-71.

Sparano A, Quesnelle KM, Kumar MS, Wang Y, Sylvester AJ, Feldman M, Sewell DA, Weinstein GS, Brose MS. 2006. Genome-wide profiling of oral squamous cell carcinoma by array-based comparative genomic hybridization. Laryngoscope 116(5):735-41.

Stein CK, Glover TW, Palmer JL, Glisson BS. 2002. Direct correlation between FRA3B expression and cigarette smoking. Genes Chromosomes Cancer 34(3):333-40.

Talamini R, Franceschi S, Barra S, La Vecchia C. 1990. The role of alcohol in oral and pharyngeal cancer in non-smokers, and of tobacco in non-drinkers. Int J Cancer 46(3):391-3.

Talamini R, La Vecchia C, Levi F, Conti E, Favero A, Franceschi S. 1998. Cancer of the oral cavity and pharynx in nonsmokers who drink alcohol and in nondrinkers who smoke tobacco. J Natl Cancer Inst 90(24):1901-3.

Taniguchi T, Garcia-Higuera I, Xu B, Andreassen PR, Gregory RC, Kim ST, Lane WS, Kastan MB, D'Andrea AD. 2002. Convergence of the fanconi anemia and ataxia telangiectasia signaling pathways. Cell 109(4):459-72.

Todd S, Franklin WA, Varella-Garcia M, Kennedy T, Hilliker CE, Jr., Hahner L, Anderson M, Wiest JS, Drabkin HA, Gemmill RM. 1997. Homozygous deletions of human chromosome 3p in lung tumors. Cancer Res 57(7):1344-52.

Tsui IF, Rosin MP, Zhang L, Ng RT, Lam WL. 2008. Multiple aberrations of chromosome 3p detected in oral premalignant lesions. Cancer Prev Res (Phila Pa) 1(6):424-9.

Van Der Heijden MS, Brody JR, Kern SE. 2004. Functional screen of the fanconi anemia pathway in cancer cells by Fancd2 immunoblot. Cancer Biol Ther 3(6):534-7.

van Zeeburg HJ, Snijders PJ, Pals G, Hermsen MA, Rooimans MA, Bagby G, Soulier J, Gluckman E, Wennerberg J, Leemans CR and others. 2005. Generation and molecular characterization of head and neck squamous cell lines of fanconi anemia patients. Cancer Res 65(4):1271-6.

Varela-Lema L, Taioli E, Ruano-Ravina A, Barros-Dios JM, Anantharaman D, Benhamou S, Boccia S, Bhisey RA, Cadoni G, Capoluongo E and others. 2008. Meta-analysis and pooled analysis of GSTM1 and CYP1A1 polymorphisms and oral and pharyngeal cancers: a HuGE-GSEC review. Genet Med 10(6):369-84.

Virgilio L, Shuster M, Gollin SM, Veronese ML, Ohta M, Huebner K, Croce CM. 1996. FHIT gene alterations in head and neck squamous cell carcinomas. Proc Natl Acad Sci U S A 93(18):9770-5.

Wang LE, Xiong P, Zhao H, Spitz MR, Sturgis EM, Wei Q. 2008. Chromosome instability and risk of squamous cell carcinomas of head and neck. Cancer Res 68(11):4479-85.

Wang X, Kennedy RD, Ray K, Stuckert P, Ellenberger T, D'Andrea AD. 2007. Chk1-mediated phosphorylation of FANCE is required for the Fanconi anemia/BRCA pathway. Mol Cell Biol 27(8):3098-108.

White JS, Weissfeld JL, Ragin CC, Rossie KM, Martin CL, Shuster M, Ishwad CS, Law JC, Myers EN, Johnson JT and others. 2007. The influence of clinical and demographic risk factors on the establishment of head and neck squamous cell carcinoma cell lines. Oral Oncol 43(7):701-12.

Wistuba, II, Behrens C, Virmani AK, Mele G, Milchgrub S, Girard L, Fondon JW, 3rd, Garner HR, McKay B, Latif F and others. 2000. High resolution chromosome 3p allelotyping of human lung cancer and preneoplastic/preinvasive bronchial epithelium reveals multiple, discontinuous sites of 3p allele loss and three regions of frequent breakpoints. Cancer Res 60(7):1949-60.

Wreesmann VB, Estilo C, Eisele DW, Singh B, Wang SJ. 2007. Downregulation of Fanconi anemia genes in sporadic head and neck squamous cell carcinoma. ORL J Otorhinolaryngol Relat Spec 69(4):218-25.

Yang Q, Yoshimura G, Suzuma T, Tamaki T, Umemura T, Nakamura M, Nakamura Y, Wang X, Mori I, Sakurai T and others. 2001. Clinicopathological significance of fragile histidine triad transcription protein expression in breast carcinoma. Clin Cancer Res 7(12):3869-73.

Zhang J, Yang PL, Gray NS. 2009. Targeting cancer with small molecule kinase inhibitors. Nat Rev Cancer 9(1):28-39.